Ultra Wideband Channel Measurements in an Indoor Office Environment with Horizontal and Vertical Polarizations

by

John A. Shields
B.Eng., University of Victoria, 2001

A Thesis Submitted in Partial Fulfilment
of the Requirements for the Degree of

MASTER OF APPLIED SCIENCE

in the Department of Electrical and Computer Engineering

© John A. Shields, 2012
University of Victoria

All rights reserved. This thesis may not be reproduced in whole or in part, by photocopy or other means, without the permission of the author.

Supervisory Committee

Ultra Wideband Channel Measurements in an Indoor Office Environment with Horizontal and Vertical Polarizations

by

John A. Shields
B.Eng., University of Victoria, 2001

Supervisory Committee

Dr. Xiaodai Dong, (Department of Electrical and Computer Engineering)
Co-Supervisor

Dr. Jens Bornemann, (Department of Electrical and Computer Engineering)
Co-Supervisor

Abstract

Supervisory Committee
Dr. Xiaodai Dong, (Department of Electrical and Computer Engineering)
Co-Supervisor

Dr. Jens Bornemann, (Department of Electrical and Computer Engineering)
Co-Supervisor

Ultra wideband (UWB) has the potential for high data rates, ranging and positioning. A UWB communication system's design requires knowledge regarding the channel. This thesis investigates the effect that different antenna orientations have on the wireless channel; in an indoor office environment. Channel reciprocity, path loss, body shadowing and spatial correlation are investigated for the frequency band 3.1 to 10.6 GHz. The measurements are performed in the frequency domain. UWB channels are shown to be highly reciprocal in all instances. Path loss versus distance was determined for line of sight (LOS) and non-line of sight (NLOS) scenarios. Body shadowing is measured for an average Caucasian male, and the root mean square (RMS) delay spread and received power loss plotted spatially. The spatial correlation is investigated using a two dimensional grid. A comparison between the horizontal and vertical polarization is made.

Table of Contents

Acronyms

EIRP	Effective isotropic radiated power
ETSI	European Telecommunication Standards Institute
FCC	Federal Communications Commission
IC	Industry Canada
LOS	Line of sight
NLOS	Non line of sight
RMS	Root mean square
UWB	Ultra wideband

List of Tables

List of Figures

Acknowledgements

There are several individuals and organizations to whom I am deeply indebted to, and without them this thesis would not have occurred. To my wife, for all your encouragements that helped me move this thesis forward. With all of your support over the years, you have made this possible. To my children, for providing the quite moments that were necessary, and the willingness to sacrifice family time. To my parents and siblings for your encouragement, help and motivation. To my employers, Daniels Electronics Ltd, and Codan Radio, for graciously allowing me to have the required time to pursue this degree. To Dr. Xiodai Dong and Dr. Jens Bornemann, for your advice and encouragement over the years. To the University of Victoria, thank you for providing the resources necessary. To God for his goodness and supporting me through this adventure.

Dedication

To my wife, for your support over the years.

1 Introduction

1.1 Historical Overview

Ultra wideband or UWB has been used since the first wireless radio frequency transmissions. Maxwell and Marconi's first spark gap emitter was essentially UWB. The spark gap emitter was used from the late 1800's to the mid 1900's. The spark gap transmitter lost popularity as FM was developed in the 1930's by Armstrong. The resulting new FM system used a much narrower bandwidth. FM had less static, was more spectral efficient. As a result the spark gap generator was abandoned. In the 1960's the sampling oscilloscope was invented and more impulse-based communications were developed. In 1998, the FCC revised part 15.209 and allowed specific companies to start developing UWB communication systems. In 2002, the FCC unlicensed the 3.1 to 10.6 GHz and other bands for UWB communication system development. The FCC defines UWB or ultra wideband as a radio technology with a bandwidth exceeding the lesser of 500 MHz or 20 percent of the arithmetic center frequency [1].

1.2 Types of UWB

There are two types of UWB signals, impulse ultra wideband (I-UWB) and, multicarrier ultra wideband (MC-UWB). I-UWB is used primarily for precision locating, and MC-UWB for secure voice and data communications. Inventory tracking is one current application where IUWB is used for both precision locating and data communications, and therefore does not fall specifically into a single FCC spectrum mask. Additional information regarding the emission masks can be obtained from [1].

The channel has a different effect on I-UWB and MC-UWB signals. In I-UWB the

bandwidth can be large and depends on the pulse's bandwidth. This greatly benefits the ability to determine the time of arrival. The drawback to the large bandwidth is that the channel can distort the signal. In MC-UWB the wide bandwidth has been divided into small sub bands. Each of these small sub bands can be made narrow enough so that the signal is not distorted. The drawback is that the effects of multipath signal combining can significantly attenuate the signal.

1.3 Research Overview

In this thesis the UWB channel is investigated within the bandwidth from 3.1 to 10.6 GHz. Channel measurements are made with a network analyzer, using bi-conical antennas, orientated vertically and horizontally, in an indoor office environment. Channel reciprocity and large scale path loss are investigated in several line of sight (LOS) and non line of sight (NLOS) environments. In two different scenarios, the received power loss is investigated with body shadowing. The spatial correlation is investigated in a single environment on a 3 x 90 grid. UWB channel measurements have been performed previously by multiple research groups. This thesis is different in that it compares the channel characteristics for vertical and horizontal antenna polarizations in an indoor office environment.

1.4 Previous Related Measurements

The indoor office environment has been previously investigated by various research groups. Measurements in both the time and frequency domain have been previously investigated. Some of that relevant research is presented in this section. Papers dealing with indoor office a UWB have been briefly summarized. In the majority of these cases

vertical polarization is used, except with measuring the angle of arrival. This thesis compares the horizontal to vertical antenna polarizations. A previous paper has been found that compares different polarizations for estimating location; the research found that the horizontal polarization offered better location accuracy [2]. This thesis adds a comparison of horizontal and vertical frequency based channel measurements in the indoor office environment.

At the University of Victoria, the UWB channel was previously investigated in the same environment using the time domain approach in the 0.38 to 4 GHz and 4 to 8 GHz ranges. Channel reciprocity, body shadowing and spatial correlation were investigated [3] [4]. The impact of the center frequency has been studied at the Moscow State University [5]. The indoor office environment in the 3.1 to 10.6 GHz bandwidth has been investigated by the Delft University of Technology, which found the amplitude fading statistics to follow a log-normal distribution, with a standard deviation decreasing linearly with the delay [6]. The Samsung Advanced Institute of Technology has investigated UWB propagation in high rise apartments at various different locations and determined the large and small scale channel statistics [7].

Body shadowing has been investigated by the University of Victoria [3]. The Tokyo Denki University has investigated the effect of both room height and positioning in a room. Tokyo Denki University determined that this only slightly affects the propagation loss and delay profiles [8]. The effect of different body postures and the effect of the floor in an indoor environment has been investigated at the Dresden University of Technology and a resulting channel model obtained using an omni directional antenna in the frequency domain from 3.1 to 10.6 GHz [9]. Signal propagation through and around

an approximate human head using a vector network analyzer in the 1.5 to 8 GHz bandwidth using omni-directional antennas has also been examined and concluded that diffraction is the main propagation mechanism around the human head [10].

1.5 Thesis Organization

This thesis is organized into five chapters. Chapter 1 is an introduction and outlines previous work by other groups. Chapter 2 reviews the characteristics of an ultra wideband channel. Chapter 3 reviews typical time domain and frequency domain channel measurement methods. Chapter 4 contains the measurements and results for reciprocity, path loss, body shadowing and small scale fading. Chapter 5 contains the conclusions and future work. The Appendix provides a list of equipment used for the measurements.

2 Characteristics of the Ultra Wideband Channel

A wireless channel is the medium between two or more antennas. The antenna is part of the wireless channel and significantly impacts the response of the channel. The spaces and objects between the antennas as well as the surroundings influence the channel's response. The objects in an office environment are passive and absorb, reflect, refract, diffract, and distort the signal. As a result of the channel the received signal is delayed due to the propagation time, contains multipaths mainly from reflected and diffracted propagation paths, and is distorted due to the antenna, and frequency dependent losses through objects.

2.1 Antenna

The antenna is a major component in the wireless channel and impacts the direction and gain of the signal. For larger bandwidths, the antenna's response becomes a concern as it can cause the signal to be significantly distorted either by frequency dependent amplitude changes or by time delays. Amplitude distortions can occur from improper impedance mismatches over frequency or by the response of the antenna. Time related distortions occur when the group delay varies with frequency and cause parts of the signal to propagate through the antenna with different delays. These dependencies also vary with the elevation and azimuth angle of the antenna. In order to achieve minimal pulse distortion, a constant gain across the desired frequency band, as well as a linear phase shift, which yields a constant group delay, is required [11]. If this is not possible, the signal can be predistorted such that the propagated signal becomes the desired signal. Since the antenna's gain and group delay may change with elevation and azimuth angle, a

predistortion correction maybe acceptable at specific angles.

2.1.1 Maximize the Effective Isotropic Radiate Power (EIRP) Across the Band

The desired effective isotropic radiated power, EIRP, is one that will maximize performance and meet the spectral emission mask [1]. The maximized EIRP across the band can be obtained by selecting a constant gain antenna or by shaping the transmitted signal to compensate for the antenna. If the transmitter and receiver are part of a two way communication link, where the antennas are being reused for both transmit and receive, then signal shaping will be required in order to meet the emission mask or to recover the signal [12].

2.1.2 Directivity

An antenna is classified as omni-directional or directional. An omni-directional antenna radiates in all directions. An isotropic antenna is an ideal omni-directional antenna that radiates equally in all directions. The gain of an antenna is relative to an isotropic antenna and is represented in dB by dBi. Typically an omni-directional antenna has a constant gain across the frequency band of interest. A directional antenna is generally larger and has a narrow beam and a large gain. A directional antenna typically does not have a constant gain across frequency. A directional antenna that is typically used to measure EIRP is a standard gain horn antenna.

The directivity of the antenna impacts the directional gain of the transmitted and or received signal. The number of multipaths received will be less with a directional than with an omni-directional antenna. The choice of the antenna depends on the system design. An omni-directional antenna is suitable when the location and directivity of the receiving and transmitting antennas are not known.

2.1.3 Group Delay

For channel measurements, the group delay of the antenna and the other equipment in the chain are critical to avoid distortions. If the group delay is not relatively constant or compensated for, the transmitted or received signal will be distorted. This distortion is caused by the frequency dependent time delay of the signal [13]. These distortions are compensated for by the network analyzer in a calibration.

2.1.4 Polarization

The polarization of the receiving and transmitting antennas needs to be considered, as misaligned polarization will result in polarization losses. There are different types of polarization, linear, horizontal, and vertical, which can also be used to create circular and elliptical polarizations. Antennas, whose fields have orthogonal polarization, will be unmatched, and as a result will not receive the desired signal. Polarization can be used to create spatially independent channels for antennas.

2.1.5 Impedance Mismatches

For channel measurements, the impedance match across a wide bandwidth is important, as it is difficult to design good ultra wide impedance matching networks. If the matches are not sufficient, the amplitude of the signal will change over frequency and will cause distortions if not compensated for. These mismatches are compensated for by the network analyzer with a calibration.

2.2 Free Space Path Loss

When a single point radiator radiates, it propagates in all directions. The radiation will then propagate radially outward. Due to spacial limitations, an antenna can only capture a

part of this energy. The loss due to the inability to capture the entire signal is referred to as the "Free Space Path Loss," (1), and is one of Friis' Laws. This free space model assumes that the transmission is in space with no interference or noise. *PL* is the path loss, P_t and P_r are the received and transmitted power, respectively. G_t and G_r are the gain of the transmitter and receiver antenna, respectively. f is the frequency in Hertz, d is the line of sight distance between the transmitter and receiver, and α is the path loss coefficient. For free space α is 2.

$$PL(f,r)=\frac{P_r(f)}{P_t(f)}=G_t(f)G_r(f)\left(\frac{\lambda}{4\pi d}\right)^{\alpha} \tag{1}$$

This equation shows that the path loss is dependent on frequency and distance. A closer look at the derivation of this equation shows where these dependencies originate. The frequency dependance originates from the receiver's antenna gain $G=4\pi A_e f^2/c^2$ [11]. The antenna's frequency dependency can be compensated if the gain of one antenna multiplied by the gain of the other antenna is proportional to the frequency squared [12], see (1).

The more general free space path loss is given in (2). Gamma, Γ, is the reflection coefficient. This equation takes into account the reflections at the transmitter and receiver antenna as well as the antenna mismatch [11].

$$PL=\frac{P_r}{P_t}=\left(1-|\Gamma_t|^2\right)\left(1-|\Gamma_r|^2\right)\left(\frac{\lambda}{4\pi d}\right)^{\alpha} G_t G_r \left|\hat{p}_t \cdot \hat{p}_r\right| \tag{2}$$

2.3 Fresnel Zone

To maximize the received signal, the region around the direct line of sight (LOS) path needs to be free from obstacles. Fresnel zone's theory specifies this based on wavelength,

λ, and distance. For a signal to be received with maximum power, the first Fresnel zone must be 60 percent unobstructed. If an obstruction covers more than 40 percent of the first Fresnel zone, the link will be considered non line of sight (NLOS). The Fresnel radius is F_n as shown in (3). For the radius of the first Fresnel zone, n = 1. The LOS distance from the antennas is d_1 and d_2 and the center frequency wavelength λ.

$$F_n = \sqrt{\frac{n\lambda d_1 d_2}{d_1 + d_2}} \tag{3}$$

2.4 Reciprocity

Reciprocity or time reversal is an important channel parameter and has been studied in various environments. Reciprocity is defined as the correlation between the channel impulse response of the transmitter to receiver and receiver to transmitter channels. A channel's forward and reverse impulse response is perfectly correlated, and 100 percent reciprocal, if the correlation is unity. Reciprocity is an important factor that can be used to simplify the receiver's design and move some of the complexity to the transmitter.

The receiver's design can be simplified, because the received impulse response can be used as a prefilter for a transmission to focus the energy spatially. This method is called time reversal and uses the complex conjugate of the channel's impulse response as the prefilter.

There are several benefits for using time reversal. First, the spatial focusing reduces the number of taps to recapture a large portion of the transmitted energy. Second, the spacial focusing decreases the RMS delay spread, which improves inter symbol interference (ISI). Equation (4) shows the correlation μ between the forward and reverse response; r_f is the forward channel response, r_r the reverse channel response.

$$\mu = \frac{\int r_f(t) \cdot r_r(t)\, dt}{\sqrt{\int r_f^2(t)\, dt \cdot \int r_r^2(t)\, dt}} \tag{4}$$

2.5 RMS Delay

The environment around us, walls, floor, ceiling, doors, furniture and living things inside an office environment affect the number of received signals, delay, phase and amplitude. Because of the environment, multiple signals are received at the receiver with varying amplitudes and delays. A smaller RMS delay indicates that the multipath energy is closer together. The RMS delay gives an indication of the potential for inter symbol interference. Significant multipaths with long delays increase the RMS delay. To avoid inter symbol interference, the symbol period needs to be much greater than the average RMS delay spread [11].

The RMS delay is the root mean square of the delayed signal, weighted proportionally to the multipath energy. τ_i is the delay of the ith received signal, *Ac(τ)* is the power delay profile and is the spatial average of the impulse response of the channel, shown in (5) [14]. The mean delay spread $\bar{\tau}$, and RMS delay spread are given in (6) and (7), respectively [15]. In these cases, the received signal $r(\tau)$ is being used as an estimate for the channel impulse response, as the measurement is being performed in frequency domain with a network analyzer and converted by a fast Fourier transform (FFT) to the time domain.

$$A_C(\tau) = |r(\tau)|^2 \tag{5}$$

$$\bar{\tau} = \frac{\sum_{i=l}^{L} \tau_i A_C(\tau_i)}{\sum_{i=l}^{L} A_C(\tau_i)} \tag{6}$$

$$\tau_{RMS} = \sqrt{\frac{\sum_{i=l}^{L} (\tau_i - \bar{\tau})^2 A_C(\tau_i)}{\sum_{i=l}^{L} A_C(\tau_i)}} \tag{7}$$

2.6 Body Shadowing

Human shadowing is an important element in the office environment, and can cause significant path loss. Shadowing occurs when someone obstructs the desired path between the transmitting and receiving antenna. The received signal changes as a result of the shadow; received signal power of the shadowed paths decrease, and additional reflections are created. The total received energy and the delay spread of the received signal will change. Typically the received power decreases, and RMS delay increases due to the lost power in the main signal. Quantifying these characteristics is important for link budget analysis and inter symbol interference calculations.

The shadowing caused by human interference can be shown with a normalized power coefficient plot, which shows the percentage of power lost or gained. The normalized power coefficient ρ is calculated by dividing the total received power $r_{x,y}$ at location x,y with body shadowing by the total received power r_0 without body shadowing, as shown in (8).

$$\rho(x, y) = \frac{\int_0^T r_{x,y}^2(t)\,dt}{\int_0^T r_0^2(t)\,dt} \tag{8}$$

2.7 Spatial Correlation

The spatial correlation characteristics of a channel are important, as they impact the performance of a system using multiple antennas. A system with multiple antennas can

use the spatial characteristics to reduce fading, interference, and increase channel capacity. Multiple input multiple output, MIMO, takes advantage of spatial characteristics to create statistically independent channels, which requires a low spatial correlation. In addition, beam formed arrays can be used to change the antenna pattern and require a high spatial correlation.

2.7.1 Total Energy

The total received energy at position *x,y* is shown in (9). The fade at a location *x,y* can be defined as shown in (10), where E_{ref} is the LOS path power without multipaths. The mean $\hat{\mu}$ and standard deviation $\hat{\sigma}$ estimates are shown in (11) and (12), respectively [11].

$$E_{x,y} = \int_0^T |r_{(x,y)}(t)|^2 \, dt \tag{9}$$

$$F_{x,y} = 10\log_{10}(E_{x,y}) - 10\log_{10}(E_{ref}) \tag{10}$$

$$\hat{\mu} = \frac{1}{N}\sum_{x,y} F_{x,y} \tag{11}$$

$$\hat{\sigma} = \sqrt{\frac{1}{N-1}\sum_{x,y}(F_{x,y} - \hat{\mu})^2} \tag{12}$$

2.7.2 Spatial Fading

Spatial fading occurs when multipaths received are not resolvable and combine destructively or constructively. The spatial fading describes the variation in the received power over a small area. UWB's large bandwidth between 3.1 and 10.6 GHz allows most multipaths to be resolvable and makes it immune to the destructive and constructive

combining at the receiver.

2.7.3 Spatial Correlation

Spatial correlation is the correlation between two or more received signals physically separated by a distance, *d*. A multipath environment is required to create low spatial correlation [16]. In narrowband channels, low spatial fading leads to a high spatial correlation. However, UWB, which has low spatial fading, can also have a low spatial correlation. This is because of the finer time resolution of UWB, as the time multipaths arrival can be resolved. The spatial correlation coefficient ρ at location *x,y* is shown in (13), where $r_{x,y}(t)$ is the received signal at time *t*, and $r_{ref}(t)$ is the reference signal at time *t*.

$$\rho(x,y)=\frac{|r_{x,y}(t)\cdot r_{ref}(t)|}{\sqrt{\int r_{x,y}^2(t)\,dt}\cdot\sqrt{\int r_{ref}^2(t)\,dt}} \tag{13}$$

3 Time and Frequency Domain Measurements

Channel measurements are necessary in order to evaluate the system performance in an environment. Measurements can be made and statistical models determined. There are two methods used to obtain the response of a channel, time domain and frequency domain. This thesis investigates the use of the frequency domain; both methods are compared and reviewed in this section.

3.1.1 Time Domain Measurements

The impulse response of the channel can be obtained using time domain techniques. The impulse ideally requires the use of the dirac-delta function. It is not possible, given the bandwidth limitations, to realize this idealistic pulse. The impulse response of the channel is estimated by sending periodic pulses over the channel. The pulses need to be separated so that all the multipath pulses are received before the next pulse is transmitted. The setup for the time domain includes a pulse generator, digital sampling oscilloscope as a wideband detector, antennas, low loss and phase stable cables, a triggering source, and a low noise broadband power amplifier. Figure 1 shows this setup. The oscilloscope's sampling period should be different from the triggering period so that different parts of the received signal are being sampled.

Timing the pulse trigger with the trigger for the oscilloscope is important in order to obtain the channel impulse response. The trigger generator should time the trigger to the pulse generator such that the pulse into the transmitting antenna arrives at the same time the oscilloscope is triggered. Jitter in the triggering pulse (either amplitude, or time) will add additional error in estimating the time of arrival.

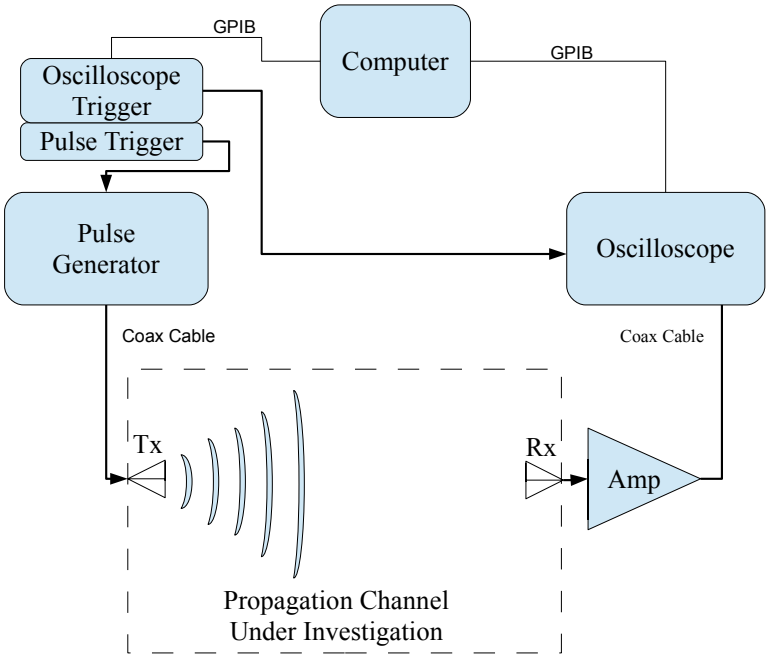

Figure 1: Block diagram of the time domain setup.

A modified approach is to use an additional antenna for triggering the oscilloscope. In this case, the added antenna is situated close to the transmitting antenna. In this setup, the delay of the cable from the antenna to the oscilloscope needs to be accounted for. This approach can be challenging as distorted and multipath components may cause the oscilloscope to be triggered multiple times. In addition, the signal level may be too low, and the additional delays may be difficult to account for.

The calibration of the time domain setup is necessary to remove the influence of the measurement equipment. The calibration of the time domain setup is performed with a calibrated attenuator. The attenuator needs to have a constant frequency response across the band as well as a linear phase. The impulse response of the channel can be obtained by deconvolving the calibrated measurement from the channel measurement [11].

For UWB there are two types of noise, narrow band and wide band. To remove narrow band noise, the time domain response can be Fourier transformed to the frequency

domain, filtered and then inverse Fourier transformed back to the time domain. Wideband noise typically consists of short pulses, and can be reduced by using averaging on the oscilloscope [11].

3.1.2 Frequency Domain Measurements

Frequency domain measurements have a couple of advantages over time domain measurements. The biggest advantage is simplicity: timing, calibration, signal sources, and impulse response are handled by the network analyzer. Network analyzers are more sensitive than oscilloscopes, which allows channels with greater path loss to be measured. The drawback to using the network analyzer is that the impulse response will be different from the deconvoluted impulse response of a time domain pulse, which would be used in a real system.

In the frequency domain, the forward gain (S_{21}) can be obtained. To measure this, the reference signal a_1 is compared to the received signal b_1 as seen in Figure 2. The DUT, device under test, is the channel, and the channel response $S_{21}=a_1/b_1$ can be determined, when the signal source a_2 is zero. Network analyzers are not designed to measure systems with large delays. When performing a calibration or measurement, the delay of the system must be considered. If the network analyzer's a_1 reference path has a delay much shorter than the path between port 1 and 2, then the phase may not be determined correctly as the reference signal a_1 maybe out of sync with the received signal b_2. To eliminate these swept errors, frequency stepped sweeping should be used instead of frequency sweeping. The delay of the frequency step should be larger than the time delay between the antennas.

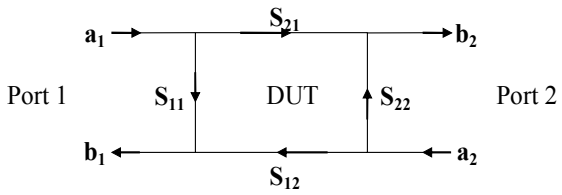

Figure 2: Block diagram of S-parameters

An estimate of the impulse response can be obtained by taking the inverse discrete Fourier transform using both the magnitude and phase of the forward gain. The inverse Fourier transform is shown in (14). The impulse response was estimated using the frequency range 3.1 to 10.6 GHz, and padding all other values to zero. The analysis shown in this thesis uses the inverse Fourier transform of the frequency domain to obtain the time domain's response.

$$f(t)=\frac{1}{2\pi}\int_{-\infty}^{\infty}(\mathcal{F}f)(x)e^{jtx}dx \tag{14}$$

The frequency domain setup requires a vector network analyzer, low loss and phase stable cables, antennas, and a low noise amplifier. In some measurement setups, the low loss cables are replaced with very low loss optical fibers with an optical modulator and demodulator. In this thesis, distances greater than 15 meters were not investigated and optical cables were not required. Figure 3 shows the frequency domain setup. To remove the antenna effects, a through calibration can be performed at a reference distance. This type of calibration was used for the measurements. Time gating was used to isolate the LOS path.

UWB was designed to work with existing systems, as such wideband noise and narrow band noise are to be expected. For narrow band noise, the frequency sweep can be segmented or selected with the appropriate stop frequencies, sweep points and intermediate frequency (IF) bandwidth. For wideband noise, averaging can be used to

reduce the noise. To measure the noise and interference, the cable connected to the transmitter antenna can be removed and connected to a 50 ohm load so that the radiation picked up by the measuring receiver is the noise [17].

4 Measurements

4.1 Setup

This section contains the setup information and results. Figure 3 shows the block diagram of the equipment setup used for the channel measurements. The channel under investigation includes the surrounding environment and the antennas. The network analyzer and controlling computer are moved away from the antennas to minimize interference with the measurement. The measurements are automated and were performed late at night or early mornings during non-office hours. This avoided unintentional interactions with the channel measurements.

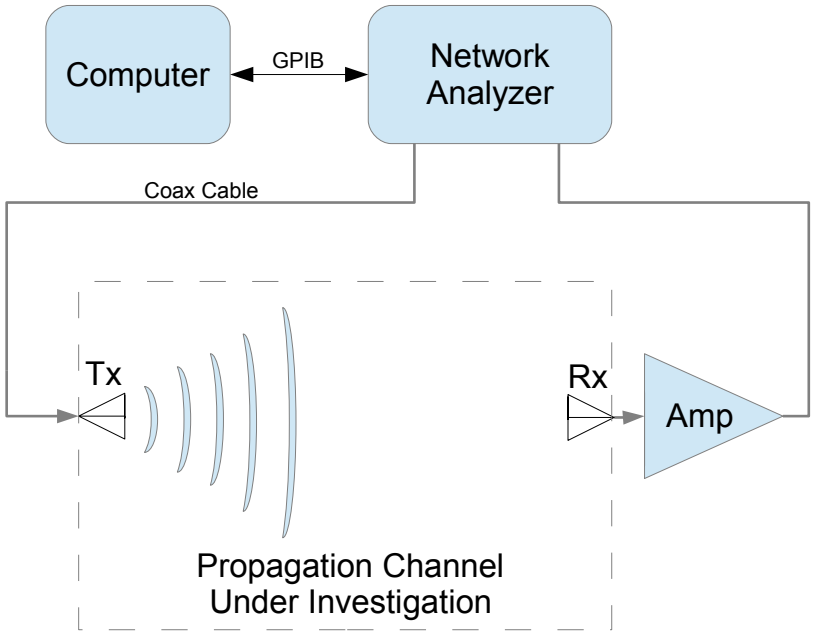

Figure 3: Block diagram of the frequency domain setup.

For further equipment information for the various channel measurements see Appendix A. The bandwidth of the network analyzer was selected to be 100 kHz as this setting gave adequate sensitivity for the measurements, and the sweep time was acceptable. The

sweep type was set to a linear step with a minimal dwell time. This was done to prevent the long propagation time of the channel from effecting the measurements. If the propagation time is too long and the dwell time too short, the network analyzer may move to the next frequency before the signal is propagated back to the network analyzer and cause an invalid measurement.

The measured propagation delay of the entire setup was checked and confirmed to be acceptable. The individual blocks were measured separately and then as a whole system. The maximum antenna separation of the system was checked to confirm that the overall electrical length of the system operated as expected. To confirm that the equipment was operating properly, the speed of light was measured by calibrating the equipment to a reference distance of 1 m and then increased to 12 m. The speed of light was calculated for a separation distance of 11 m, to be $3.00 \times 10^8 \pm 0.63\%$ using the $v=d/t$, where v is the velocity and in this case the estimate for the speed of light, d is the distance, and t is the time. The above measured speed of light is within error of the speed of light in air at standard temperature and pressure.

4.1 Scenarios

The indoor wireless measurements were performed at the University of Victoria's Engineering Office Wing in the 3rd floor's wireless lab. Figure 4 shows the locations for the various different scenarios where the measurements were taken. The x, y, and z axes are shown in the figure and are used to specify the orientation and movement of the antennas in the measurements. The z axis is out of the page or towards the ceiling in the lab, and is referred to as the vertical polarization. The horizontal polarization of the antenna is specified as either along the x or y axis.

The building is constructed of concrete with glass windows around the exterior. The building's internal walls are framed with metal studs and covered with drywall. The floor is concrete, as is the floor above. The ceiling is made out of ceiling tiles with an air space above for utilities. The floor is carpeted with a low pile carpet. The location of the desks and chairs may not be as shown.

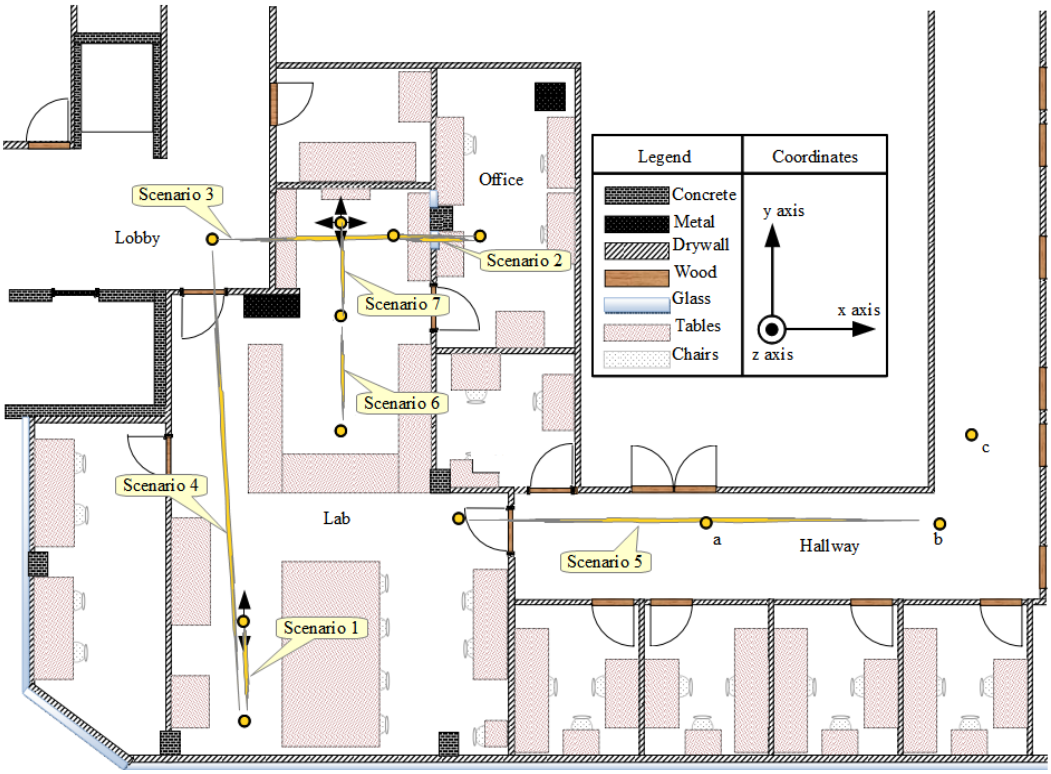

Figure 4: UVic's 3rd floor engineering office wing lab and surrounding rooms.

4.2 Reciprocity

The channel reciprocity measurements were performed with a bi-conical omni-directional antenna in different office environments, and with different antenna orientations. Measurements were performed with the antenna orientated vertically and horizontally, creating vertical and horizontally polarized waveforms. LOS and NLOS environments were investigated. The measurement distance extends from less than 1

meter to over 12 meters. In each case the reciprocity was measured. A 1 meter LOS time gated measurement is used as a reference. The measurements were performed with the antennas remaining in a fixed location, and the coax cables to the antennas reversed to perform the forward and reverse measurement. S_{12} could not be measured directly due to the reverse isolation of the amplifier.

4.2.1 Vertical Polarization Results

4.2.1.1 Reciprocity in a LOS Environment

A LOS measurement with the antennas orientated along the z axis or with vertical polarization were performed in scenario 1 as shown in Figure 4. The distance between the two antennas was varied along the y axis between 0.9 to 4.2 meters. The elevation from the carpeted concrete floor, or z as shown in Figure 4, was kept constant at 1 meter. The results in Table 1 show the correlation between the forward and reverse link of the LOS channel in scenario 1 with vertical polarization. The results show that the reciprocity of the channel in a static, LOS, constant height environment is consistently 1.0.

Distance (m)	Correlation
0.9	1.0
1.2	1.0
1.5	1.0
1.8	1.0
2.1	1.0
2.4	1.0
2.7	1.0

3.0	1.0
3.3	1.0
3.6	1.0
3.9	1.0
4.2	1.0

Table 1: LOS reciprocity at various distances at scenario 1 with vertically polarized antennas.

4.2.1.2 Reciprocity With Diffraction

The next environment investigated is scenario 2 as shown in Figure 4. Again the orientation of the antenna is in the z axis. This is a LOS through a window with a metal frame and metal framed wall. This structure was used to create many multipaths. The antenna's location remains fixed in the x axis, and the elevation z varied. The antennas remain a fixed 1.5 meters away from the window along the x axis. Figures 5 through 7 show the forward and reverse link for three different variations in the z axis. Figure 5 and 7's first received path has more loss than Figure 6, as the main path is through the wall and/or window frame. Figure 5 and 7 also have more multipaths, which is due to diffraction occurring around the window frame and metal studs. Figure 6's first received path is significantly larger as the main path is through the glass window pane. Table 2 shows the results and correlation between the forward and reverse link of the channel in scenario 2 with vertical polarization. The results show that the reciprocity of the channel in a static environment is greater than 0.99.

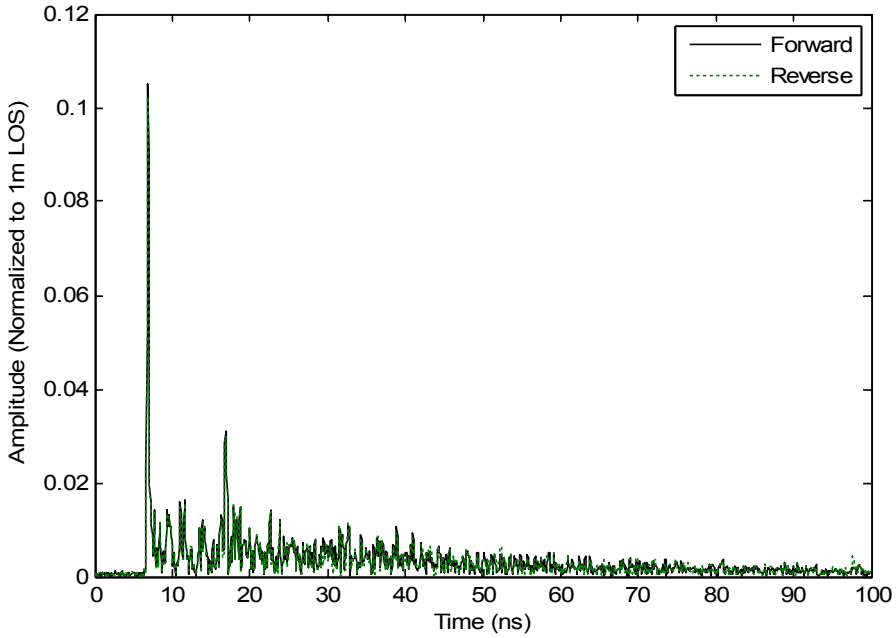

Figure 5: NLOS reciprocity at scenario 2 with vertical polarized antennas, and the lab and office antenna heights are at a 1.0 meter elevation.

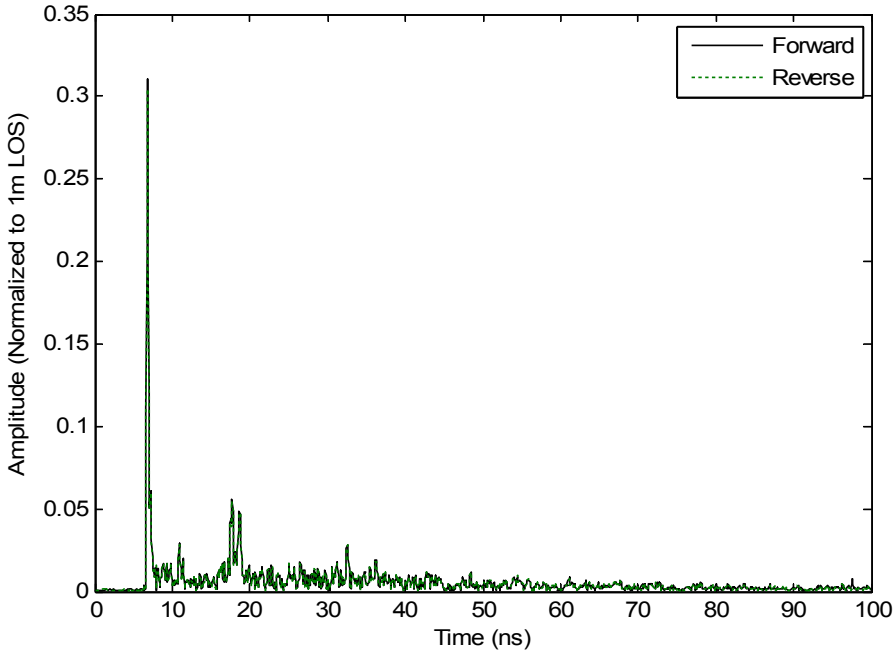

Figure 6: NLOS reciprocity at scenario 2 with vertical polarized antennas, and the lab and office antenna heights at 1.0 and 1.4 meter elevation, respectively.

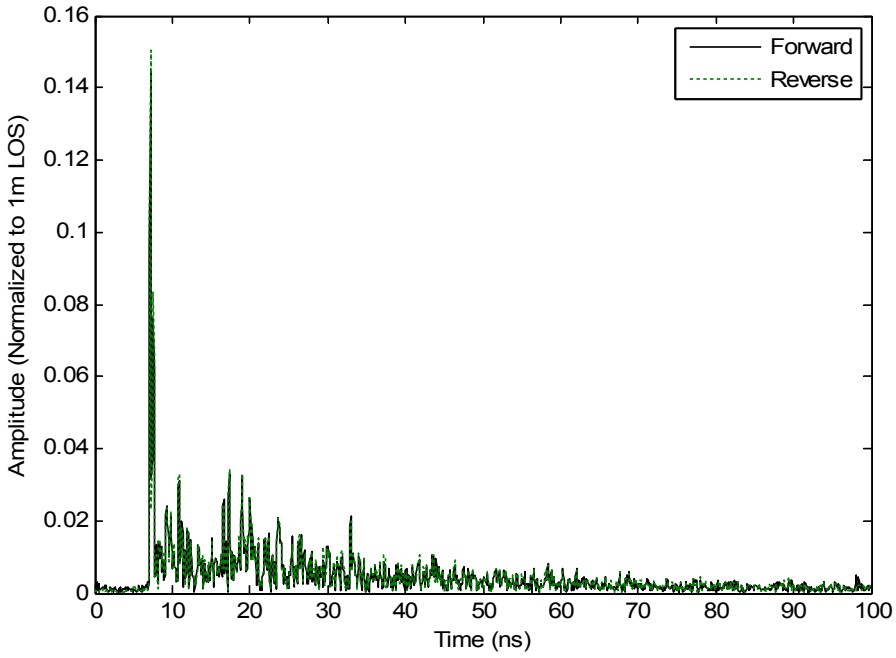

Figure 7: NLOS reciprocity at scenario 2 with vertical polarized antennas, and the lab and office antenna heights at 1.0 and 2.0 meter elevation respectively.

Lab Antenna Elevation (m)	Office Antenna Elevation (m)	Description	Correlation
1.0	1.0	NLOS through metal frame	0.99
1.4	1.0	NLOS through Window	1.0
2.0	1.0		1.0

Table 2: Reciprocity at various elevations with diffraction at scenario 2 with vertically polarized antennas.

4.2.1.3 Reciprocity In Environments With Significant Path Loss

The correlation between the forward and reverse channels was previously investigated in the same office environment using the same antennas and amplifier but using an

oscilloscope as the receiver [4]. Due to the limited sensitivity of the oscilloscope and the setup used, channels that have significant path loss either due to antenna separation distance or obstructions were not possible. A network analyzer's sensitivity is better, and with using the same cables and low noise amplifier, is able to detect a weaker signal. The scenarios below exhibit significant path loss due to obstructions or have separation distances that are greater than have previously been measured [4].

The next environment investigated is the reciprocity in scenario 3 as shown in Figure 4. This is a NLOS path through two walls one with the metal window frame previously examined, and the other with kitchen style cupboards and counter with drawers below. The vertical antenna orientation is along the z axis. The distance between the two antennas in the x axis is constant. The z elevation of the antenna in the lobby is constant at 1 meter, and the elevation of the antenna in the office varied. A reference measurement was performed with a 1 meter height and separation.

This channel offers significant path loss and multipaths, as can be seen in Figure 8 and 9. Figure 9 is also interesting as the first received path is not the largest. The field strength in Figure 9 is larger than in Figure 8 because there is less loss through the pane of glass then the metal window frame. The similarities between the forward and reverse link is evident in Figures 8 and 9. The correlation between the forward and reverse link are shown in Table 3. In all cases the correlation is 0.99, which shows that the forward and reverse links are very highly correlated.

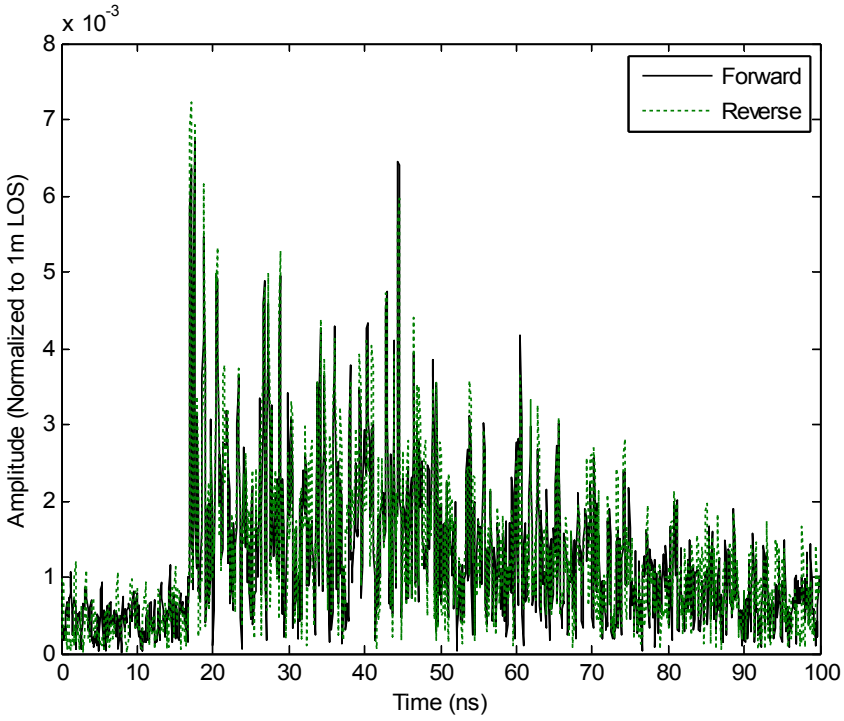

Figure 8: NLOS reciprocity at scenario 3 with vertical polarized antennas, and the lobby and office antenna heights are at a 1.0 meter elevation.

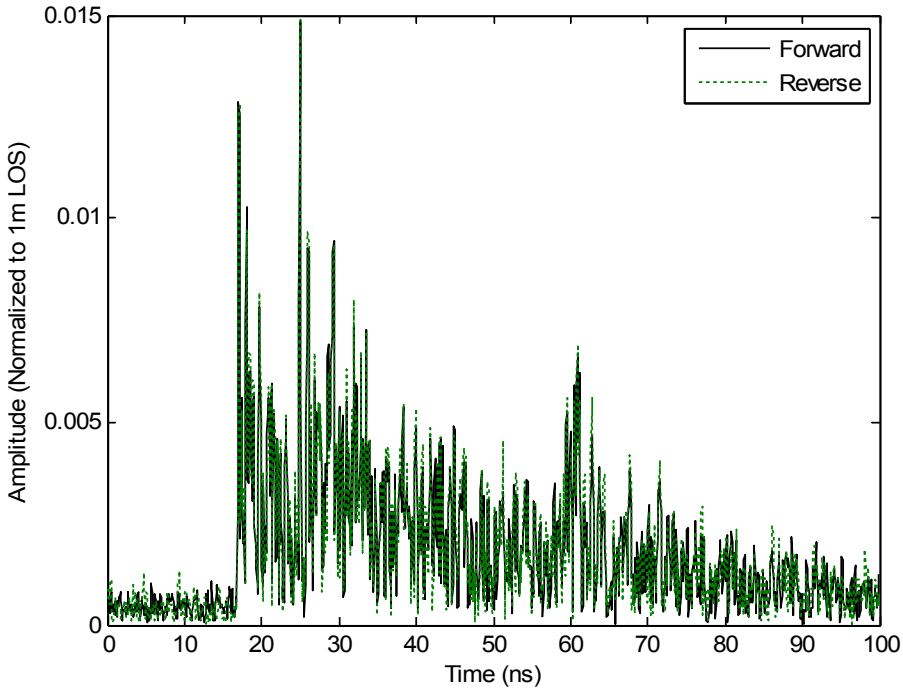

Figure 9: NLOS reciprocity at scenario 3 with vertical polarized antennas, and the lobby and office antenna heights at a 1.5 and 1.0 meter elevation, respectively.

Lab Antenna Height (m)	Lobby Antenna Height (m)	Description	Correlation
1.0	1.0	Through metal frame cupboards & wall	0.99
1.5	1.0	Through window, cupboards & wall	0.99
2.0	1.0		0.99

Table 3: NLOS Reciprocity at various elevations with diffraction and significant path loss at scenario 3 with vertically polarized antennas.

Due to the output power limitations by FCC and IC for UWB, the maximum useable distance is 10 m [18]. The next environments investigated are at distances greater than 10 meters. This is performed to investigate if the correlation between the forward and reverse links degrades as the distances increases. Scenario 4 and 5 investigate path lengths greater than 10 meters.

The next environment investigated is scenario 4. The antennas are separated by 12 meters along the y axis in a LOS and NLOS environment. The antennas are orientated along the z axis with a 1 meter elevation. The difference between the LOS and NLOS is with the solid core door opened and closed. The forward and reverse received NLOS path is show in Figure 10. The correlation between the forward and reverse paths is 1.0 as show in Table 4.

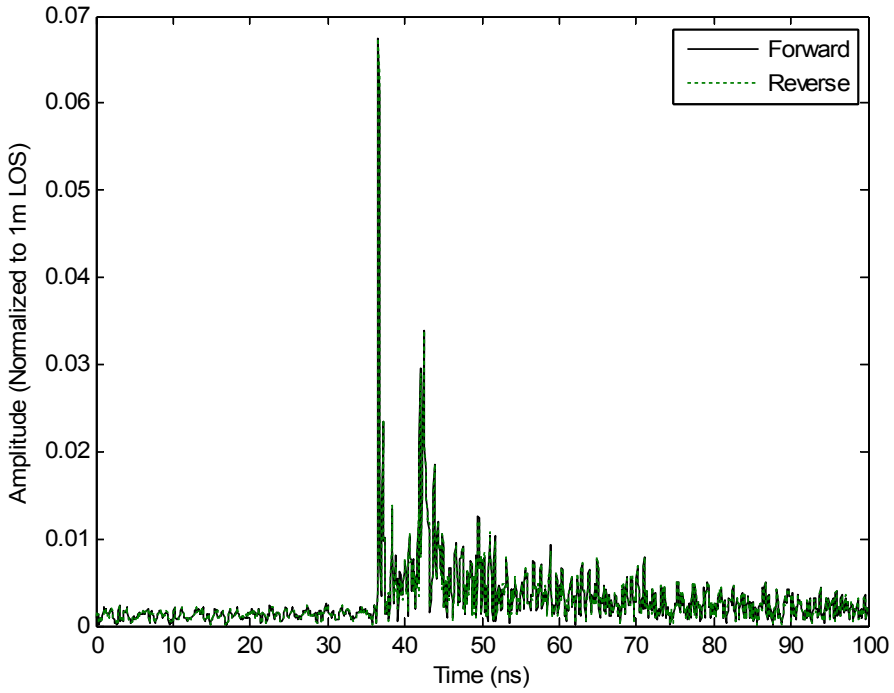

Figure 10: NLOS reciprocity at scenario 4 with vertical polarized antennas separated by 12 meters with an elevation of 1.0 meter.

Distance (m)	LOS	NLOS
12	1.00	1.00

Table 4: LOS / NLOS reciprocity with a 12 meter separation at scenario 4 with vertical polarization.

In scenario 5, a hallway environment is investigated, which can provide a lossy waveguide, as the signals reflect off the walls in a lossy manner. If the hallway were constructed out of a perfect conductor, then it would be considered a lossless waveguide. The reciprocity down a hallway with separation distances of 5, 10 and 13 meters are investigated. The antennas are orientated along the z axis, with a 1 meter elevation. In this case the hallway was constructed of drywall and metal studs. The forward and reverse channels of the NLOS path at 10 meters is shown in Figure 11, and the NLOS

path at 10 meters plus 3 meters around the corner of the hall is shown in Figure 12. The correlation, between the forward and reverse links are shown in Table 5 and are greater than or equal to 0.97, thus highly correlated.

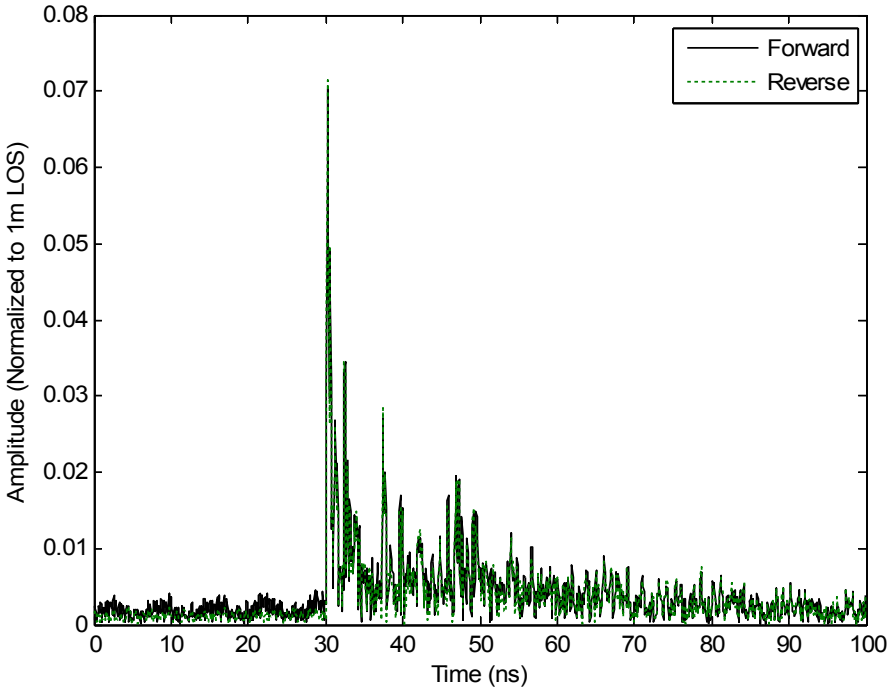

Figure 11: NLOS reciprocity at scenario 5 with vertical polarized antennas separated by 10 meters with an elevation of 1.0 meter.

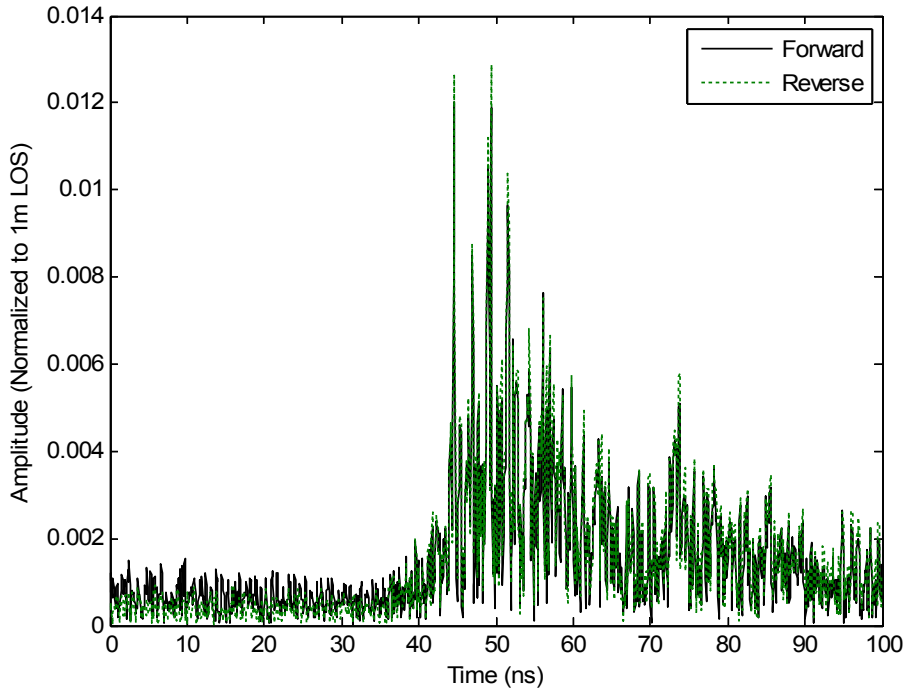

Figure 12: NLOS reciprocity at scenario 5 down the hallway and around the corner with vertical polarized antennas separated by 10 + 3 meters with an elevation of 1.0 meter.

Distance (m)	LOS	NLOS
5	0.99	0.99
10	0.97	0.99
10 + 3 around the corner	N/A Not LOS	0.99

Table 5: LOS / NLOS reciprocity with various separations at scenario 5 with vertical polarization.

4.2.2 Horizontal Polarization

The measurements that were performed previously in the same environment in the time domain were performed with the antenna in a vertical orientation [4]. This section investigates the measurements performed in Section 4.2.1 but with the antenna orientated horizontally. To distinguish the horizontal orientation of the antenna, the axis shown in

Figure 4 is used to specify if the antenna is orientated along the x or y axis. The elevation of the center of the antenna is set to be 1 meter off the carpeted concrete floor unless otherwise specified.

4.2.2.1 LOS

The LOS in scenario 1 was measured with the antenna orientated along the -x axis. The results in Table 6 show that the forward and reverse links are highly correlated, 1.0.

Distance (m)	Correlation
0.9	1.0
1.2	1.0
1.5	1.0
1.8	1.0
2.1	1.0
2.4	1.0
2.7	1.0
3.0	1.0
3.3	1.0
3.6	1.0
3.9	1.0
4.2	1.0

Table 6: LOS reciprocity at various distances at scenario 1 with horizontally polarized antennas.

4.2.2.2 Reciprocity With Diffraction

Scenario 2 as shown in Figure 4 was again used to achieve a multipath environment, using the metal window frame to create diffractions. The setup was the same except that the antennas are orientated along the y axis. The forward and reverse paths of the channel

are shown in Figures 13 to 15. Figure 13 contains significant multipaths, created by the metal window frame and supporting metal studs. Figure 14 and 15 do not have as many multipaths, as there is a path through the glass, and the diffractions around the window frame have significant affect on the path loss. The correlation between the forward and reverse paths is shown in Table 7, and is highly correlated, 1.0.

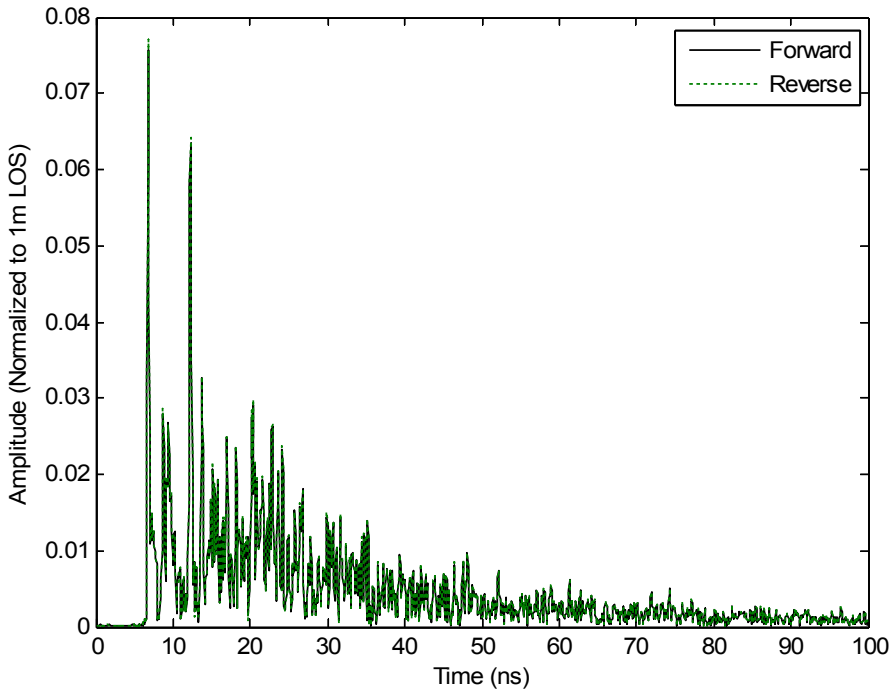

Figure 13: NLOS reciprocity at scenario 2 with horizontal polarized antennas, and the lab and office antenna heights are at a 1.0 meter elevation.

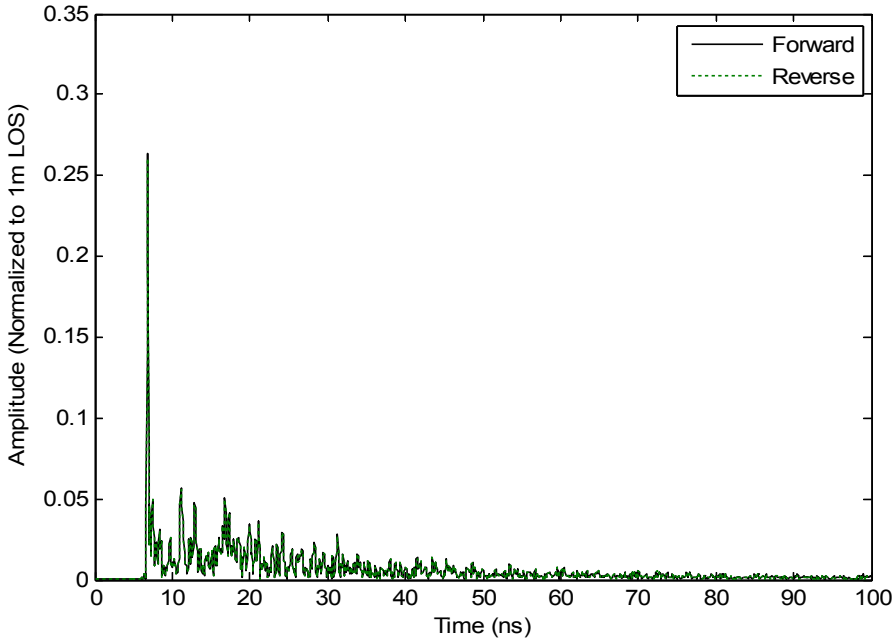

Figure 14: NLOS reciprocity at scenario 2 with horizontal polarized antennas, and the lab and office antenna heights at 1.0 and 1.4 meter elevation, respectively.

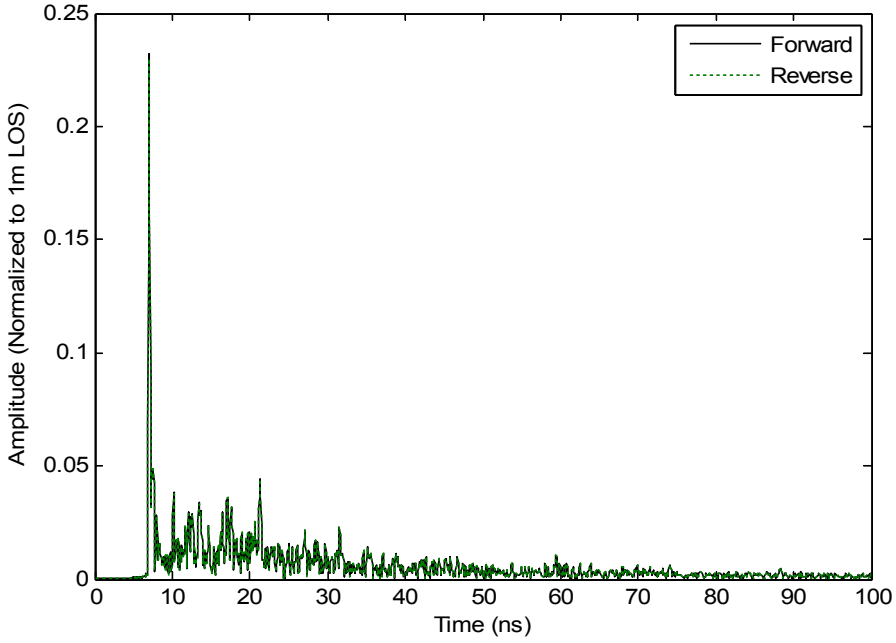

Figure 15: NLOS reciprocity at scenario 2 with horizontal polarized antennas, and the lab and office antenna heights at 1.0 and 1.8 meter elevation, respectively.

Lab Antenna Height (m)	Office Antenna Height (m)	Description	Correlation
1.0	1.0	LOS through metal frame	1.0
1.4	1.0	LOS through Window	1.0
1.8	1.0		1.0

Table 7: Reciprocity at various elevations with diffraction at scenario 2 with horizontally polarized antennas.

4.2.2.3 Reciprocity In Environments With Significant Path Loss

Scenario 3 as shown in Figure 4 was investigated with the antennas orientated along the negative y axis. The antenna elevation in the office is varied at 1.0, 1.4 and 1.8 meters off the floor. The antenna elevation in the lobby is kept constant at 1.0 meters. Again this is a NLOS channel with significant multipaths and path loss. The forward and reverse links are shown in Figure 16 and Figure 17. Figure 17 is particularly interesting as there are two significant paths that are significantly spaced. The second significant path length is at least 3 times as long as the first received path. The correlation between the forward and reverse path for the three different heights is shown in Table 8 and is highly correlated, 1.0.

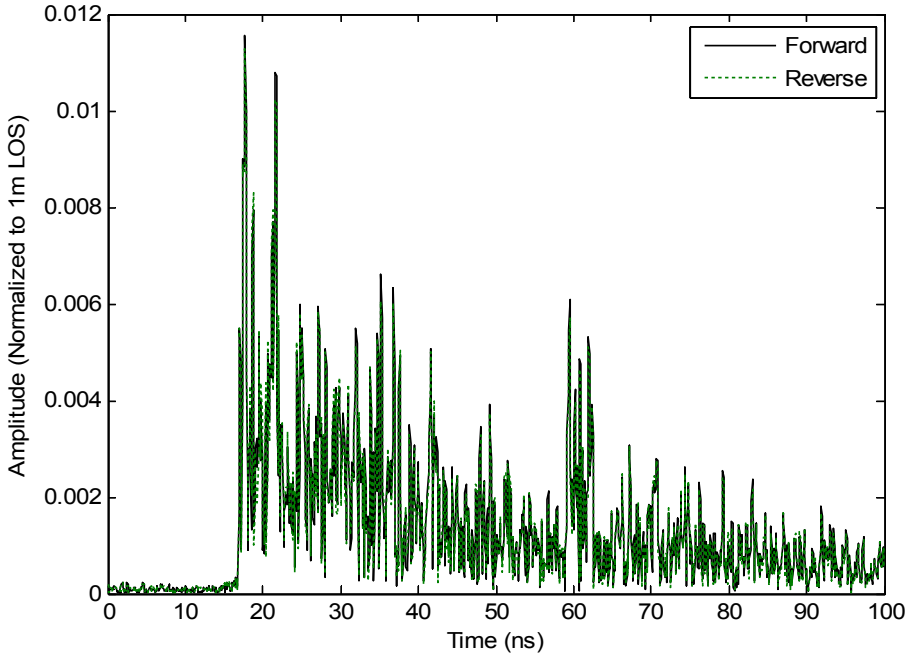

Figure 16: NLOS reciprocity at scenario 3 with horizontal polarized antennas, and the lobby and office antenna heights are at a 1.0 meter elevation.

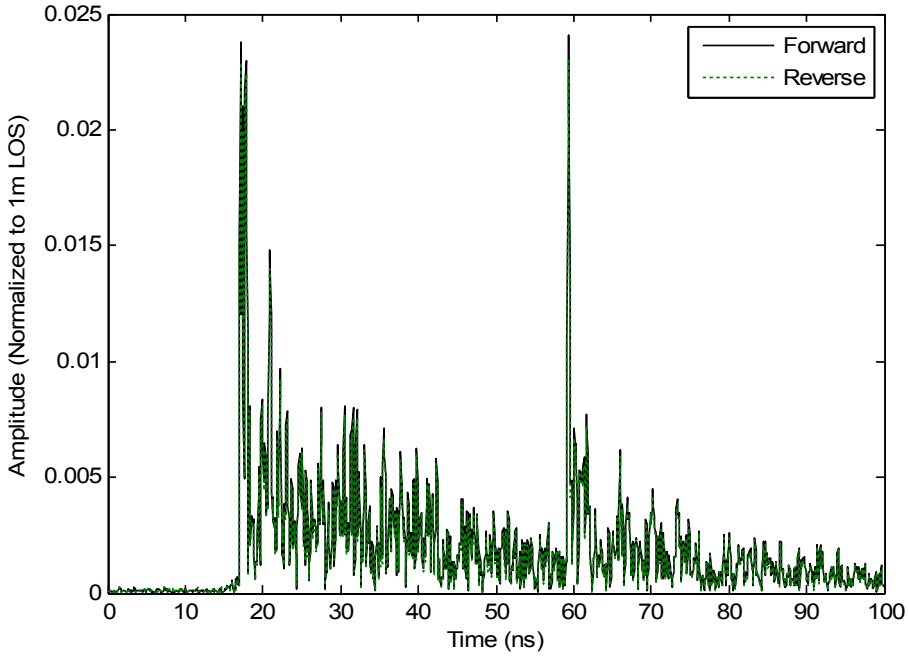

Figure 17: NLOS reciprocity at scenario 3 with horizontal polarized antennas, and the lobby and office antenna heights at a 1.4 and 1.0 meter elevation, respectively.

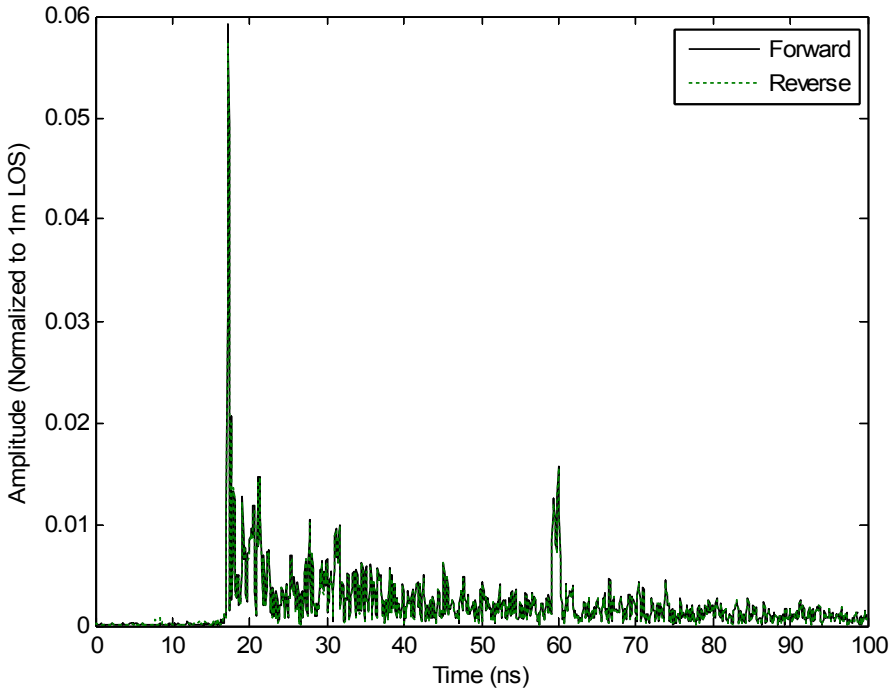

Figure 18: NLOS reciprocity at scenario 3 with horizontal polarized antennas, and the lobby and office antenna heights at a 1.8 and 1.0 meter elevation, respectively.

Reciprocity with Diffraction Scenario 3 through window with metal frame			
Office Antenna Height (m)	Lobby Antenna Height (m)	Description	Correlation
1.0	1.0	Through metal frame cupboards & wall	1.0
1.4	1.0	Through window, cupboards & wall	1.0
1.8	1.0		1.0

Table 8: NLOS Reciprocity at various elevations with diffraction and significant path loss at scenario 3 with horizontally polarized antennas.

The reciprocity of the forward and reverse channels for horizontal polarization with distances greater than 10 meters is investigated. The antennas are orientated along the y axis. The two scenarios investigated are, scenario 4 and scenario 5 as shown in Figure 4. The NLOS is created by closing the solid wooden door to the lab. The first scenario investigated is scenario 4. The forward and reverse channel response for the NLOS is show in Figure 19. The correlation between the forward and reverse paths is shown in Table 9 and is highly correlated, 1.0. The second scenario investigated is scenario 5, propagation down the hallway. The measurements are performed at 5 and 10 meters in a LOS and NLOS environment. Additional measurements are performed down the hall and around the corner at 10 + 3 meters. The orientation of the antennas remains constant until the last item in Table 10. In this case the hall antenna's orientation changes along the x axis. The forward and reverse channel responses for the NLOS at 10m, around the corner, and around the corner with the antenna orientated along the x axis are shown in Figure 19 to 22, respectively. The correlations of the forward and reverse paths are shown in Table 10 and are highly correlated, with at least 0.97 in this significantly attenuated channel.

Distance (m)	LOS	NLOS
12	1.00	1.00

Table 9: LOS / NLOS reciprocity with a 12 meter separation at scenario 4 with horizontal polarization.

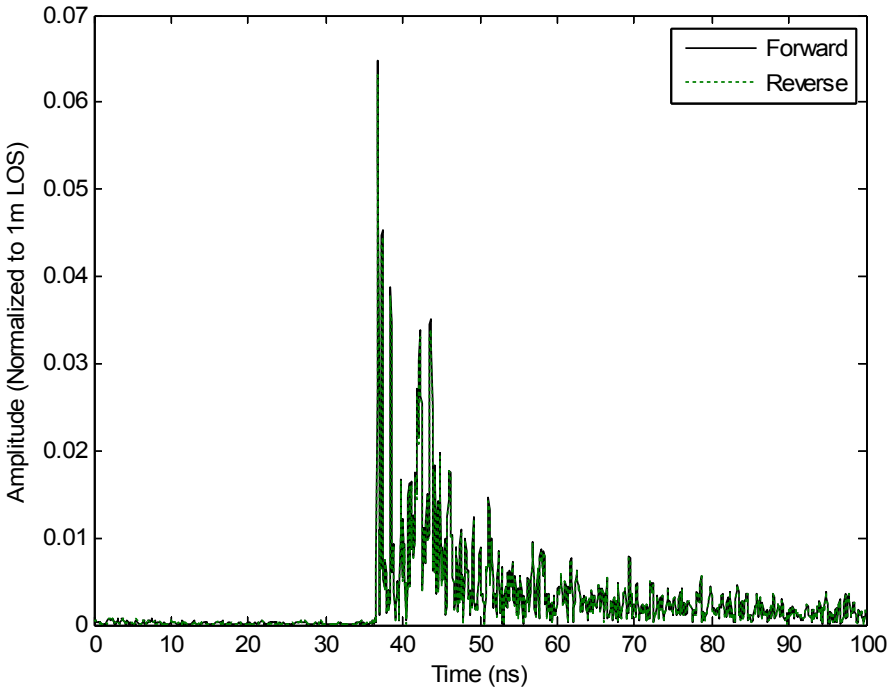

Figure 19: NLOS reciprocity at scenario 4 with horizontal polarized antennas separated by 12 meters with an elevation of 1.0 meters.

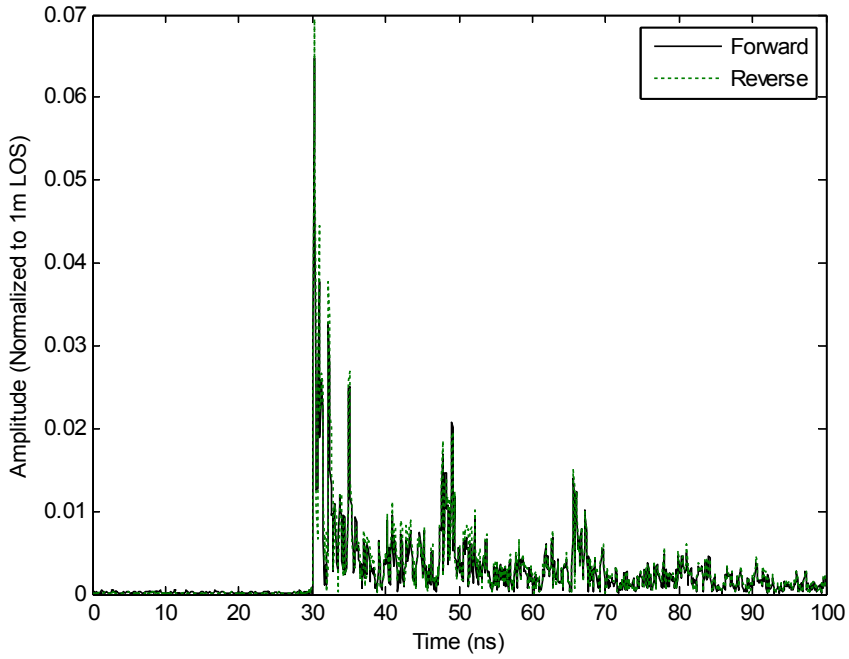

Figure 20: NLOS reciprocity at scenario 5 with horizontal polarized antennas separated by 10 meters with an elevation of 1.0 meters.

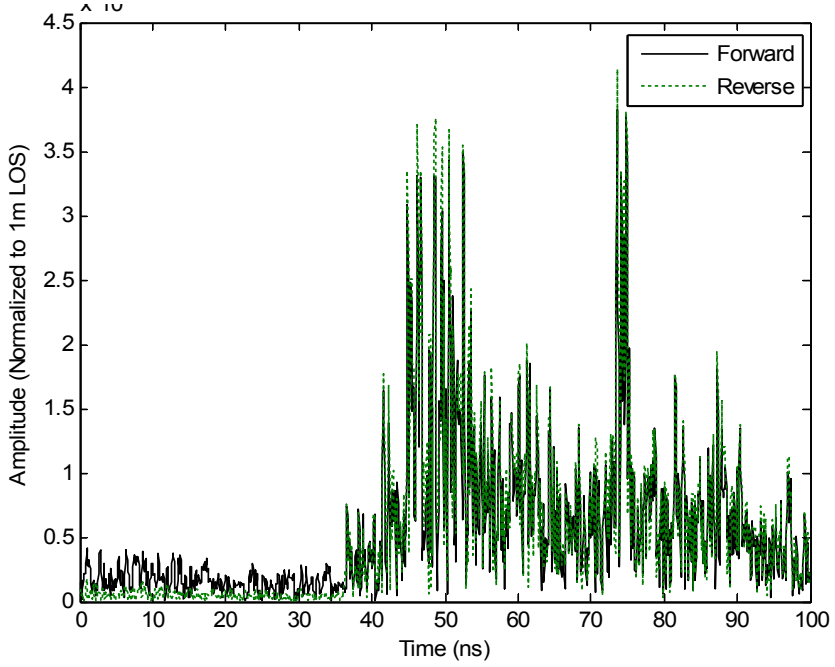

Figure 21: NLOS reciprocity at scenario 5 down the hallway and around the corner with horizontal polarized antennas separated by 10 + 3 m with an elevation of 1 m.

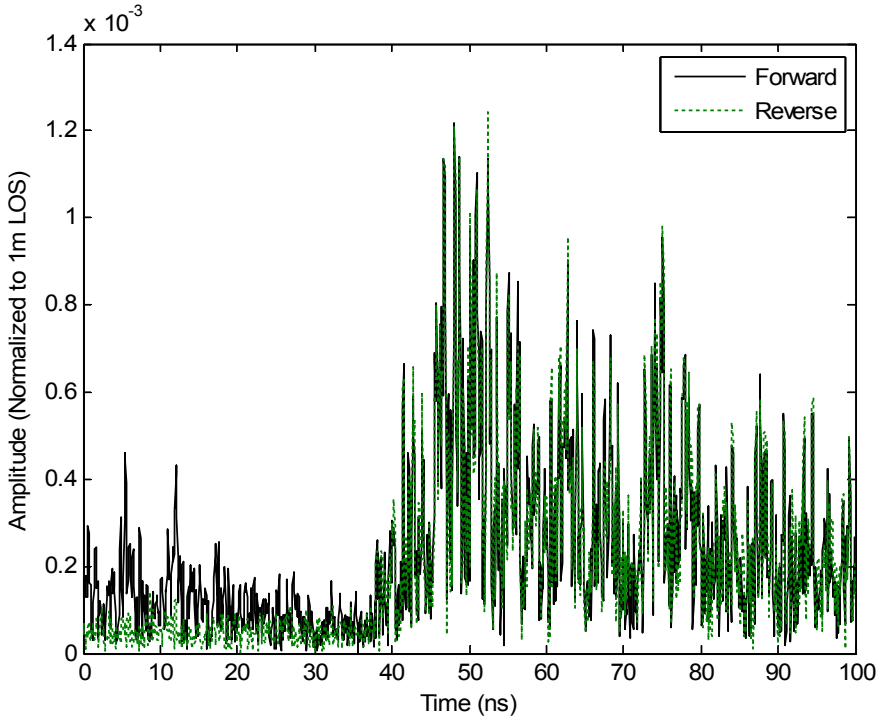

Figure 22: NLOS reciprocity at scenario 5 down the hallway and around the corner with horizontal polarized antennas along the x, y axis separated by 10 + 3 m with an elevation of 1 m.

Distance (m)	LOS	NLOS
5	0.99	0.99
10	0.99	0.99
10 + 2 around the corner	N/A	0.98
10 + 2 around the corner (scene 6 antenna orientated y axis, hall antenna orientated -x axis)		0.97

Table 10: LOS / NLOS reciprocity with various separations at scenario 5 with horizontal polarization.

4.2.3 Unmatched Polarization

In a real scenario the polarization of the antennas will likely not be perfectly matched, and it is also likely that the antennas will be at different heights. This will cause the angle of arrival and the polarization to change at various heights and angles. To test the reciprocity at various angles and heights, one antenna was kept constant, with the antenna orientated in the z axis, while the other antenna varied in height and angle from the z axis. The channel is measured in scenario 6, as shown in Figure 4. The LOS distance between the antennas was kept relatively constant. The forward and reverse channel correlation are shown in Table 11. The channels are highly correlated at 0.99.

Variable Height (m)	Angle (degrees) from vertical axis	Correlation
1.0	0	0.99
1.4	44	0.99
2.0	54	0.99

Table 11: LOS reciprocity with antenna polarization mismatch

4.2.4 Reciprocity Conclusions

The forward and reverse paths were investigated and furthered the measurements already performed previously in the same environment using the time domain [4]. One of the trade-offs to using an oscilloscope as opposed to network analyzer is that the sensitivity of the equipment limits the path loss that can be measured. The network analyzer is much more sensitive which allows it to detect weaker signals. As a result, the correlation between the forward and reverse paths were investigated at distances greater than previously performed. The same equipment was used, not including the source and detector. Channels with significant path loss were also investigated. In an indoor office environment this also means that the received power is spread out over time. Antenna separation distances greater than 10 meters were investigated, to ascertain if the reciprocity would degrade.

Antenna orientation was also considered. Measurements were performed with the antenna orientated vertically and horizontally in the same scenarios. Some additional cross polarization measurements were also performed. All measurements performed conclude that the correlation between the forward and reverse paths was at worst 0.97 and in most cases 0.99 or 1.0. This indicates that the forward and reverse channels can be considered reciprocal with a correlation of at least 0.97.

4.3 Large Scale Path Loss Comparison for Different Scenarios

The path loss is an important aspect when designing a communication system, and is a function of distance, obstructions, and antennas. Using Friis' free space path loss, the path loss can be calculated using (15). The path loss coefficient α, is calculated using the received power in the first received path for the scenarios shown in Table 11. LOS and NLOS paths were measured, as well as with antennas with vertical and horizontal polarization. The path loss in (15) is the additional path loss relative to the reference distance d_0.

$$PL_{d_0} = 10\,\alpha \log\left(d / d_0\right) \tag{15}$$

4.3.1 Simple Receiver Path Loss

In a simple receiver design, the first significant path is used, or the first tap. The data collected in scenarios 1 through 5 are analyzed to determine the path loss. The LOS path loss coefficient shown in Table 12 varied from 1.9 to 2.4. The NLOS path loss shown in Table 13 varied from 2.1 to 4.6 depending on the environment. Scenario 3 provided the most path loss as the path was through two walls with a path loss coefficient between 4.8 and 3.1. The similar scenario 2 provided a path loss between 4.6 and 2.6.

Scenario	Distance (m)	Path Loss coefficient α	
		Vertical	Horizontal
1	1.2	2.4	2
	1.5	2.1	2.2
	1.8	2	2.3
	2.1	2.1	2.1
	2.4	2.1	2.2
	2.7	2	2.2
	3	2.1	2.1
	3.3	2.1	2.1
	3.6	2.1	2.1
	3.9	2.1	2.2
	4.2	2	2.1
4	12	2	1.9
5	5	2	2.2
	10	2	2.1

Table 12: The path loss coefficient of the first received path in various LOS environments with the antennas orientated horizontal and vertical.

Scenario	Distance (m)	Path Loss coefficient α	
		Vertical	Horizontal
2	3	4	4.6
	3	2.1	2.4
	3.1	3.3	2.6
3	6.1	5.6	4.8
	6.1	4.8	4.1
	6.2	3.2	3.1
4	12	2.2	2.2
5	5	2.5	2.4
	10	2.4	2.3

Table 13: The path loss coefficient of the first received path in various NLOS environments with the antennas orientated horizontal and vertical.

4.4 Body Shadowing

In body shadowing, the path loss caused by humans interacting with the channel is investigated. The body shadowing measurements were performed in location 1 and 6, which is shown in Figure 4. The measurements are performed on a grid, which is shown in Figure 23. A 7 x 14 grid is used with a grid spacing of 0.3 meters. The elevation of the antennas is 1 meter off the floor. The measurements are referenced to a 1 meter LOS. Each end of the grid has an antenna which remains fixed. The interfering person is orientated facing the transmit antenna at location (0,4) which is shown in Figure 23. Channel measurements are performed with the person at each of the intersections of the grid. As this is not a real time measurement, the person during the measurement is as stationary as possible.

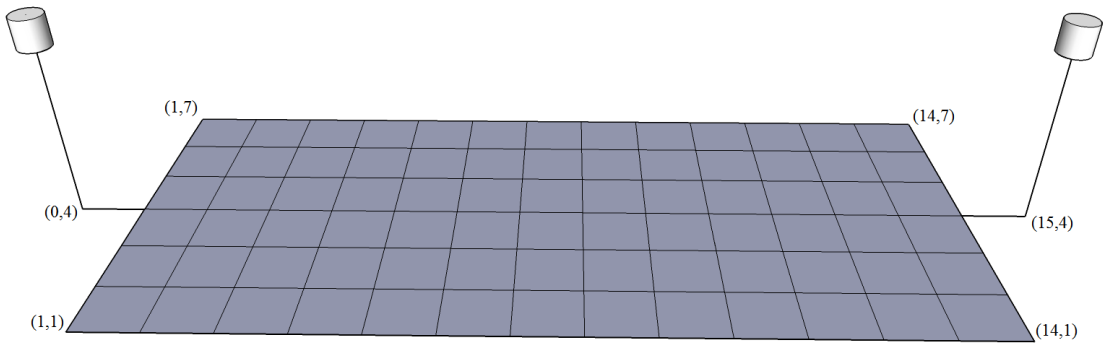

Figure 23: Body shadowing measurement grid

4.4.1 Body Shadowing Power 0.38 to 4 GHz

Previously, body shadowing was investigated using the time domain, with a pulse generator. The frequency bandwidth of the pulse was 0.38 to 4 GHz [4]. This measurement was performed as a comparison, using the frequency domain in the same location of the lab [3]. This location corresponds to scenario 1 as shown in Figure 4. The antennas were orientated vertically. The height and weight of the person used previously is unspecified, as well if the person is facing the transmit or receive antenna, and exactly how they are orientated in the path [3]. It is assumed from Figure 3 listed in [3] that the feet are centered around the intersection of the coordinates, and are slightly separated. A 160 pound, 6 foot male was used to perform the measurement. The measurement was centered around waist height, the human under test was wearing jeans and a t-shirt, shoes, a belt with metal belt buckle and pocketing an iphone, 250g of keys and a large wallet. The details of the prior measurement are not known.

The channel response of the channel with and without body shadowing at location (4,7) is show in Figure 24. As can be seen, the path loss of the first received path, or the main

LOS path, is attenuated by the body shadowing. The second main path is the ground reflection and is also attenuated, even with the feet slightly apart. Other paths are not significantly attenuated, unless the path is also obstructed by the body. There is a slight delay of 0.1 ns of the first received path between the body shadowed path and unobstructed path which is caused by the propagation delay through the body. The first received path with body shadowing is 30% of the non-obstructed, calculated from the data plotted in Figure 24. The correlation between the paths with no body shadowing and with body shadowing at location (4,7) is 0.90. If the first received path is removed, as this is the path that has most of the signal degradation from the analysis, the correlation between the non obstructed and body shadowed path increases to 0.94. Both are highly correlated.

Figure 25 shows the normalized power coefficient of the entire received signal, normalized to the received signal without body shadowing. The energy at the middle of

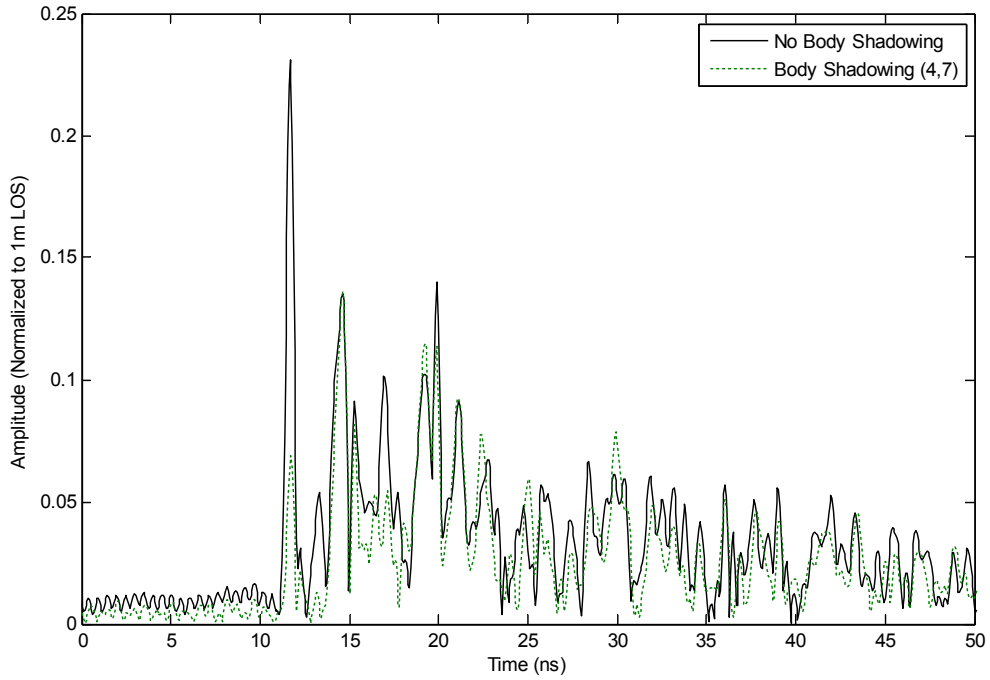

Figure 24: Correlation with and without body shadowing in scenario 1 of the received signal, with a bandwidth of 0.38 – 3.8 GHz and the antennas orientated vertically.

the LOS path, coordinates (4,7) is 60% of the power without body shadowing. The body shadowing has minimal degradation on the received energy when the body is 0.6 meters away from the LOS path. Additional energy may be reflected to the receiving antenna as seen in Figure 25 at coordinates (7,6), (9,6), (6,2), (7,2) and (9,2) where the received power is greater than that without body shadowing. The prior measurement performed in the time domain [3] measured the energy attenuation in the middle of a similar setup to be 90% of the power without body shadowing. There were also no points where the received signal energy was more than that without body shadowing. The discrepancies may be in part related to the height, weight, size, clothing and other personal items either worn or in pocket. However it is likely that the differences are related to the differences between the time domain pulse and the frequency domain's impulse response. In addition

to these the office clutter and furniture had changed somewhat since the measurement in [3] was performed.

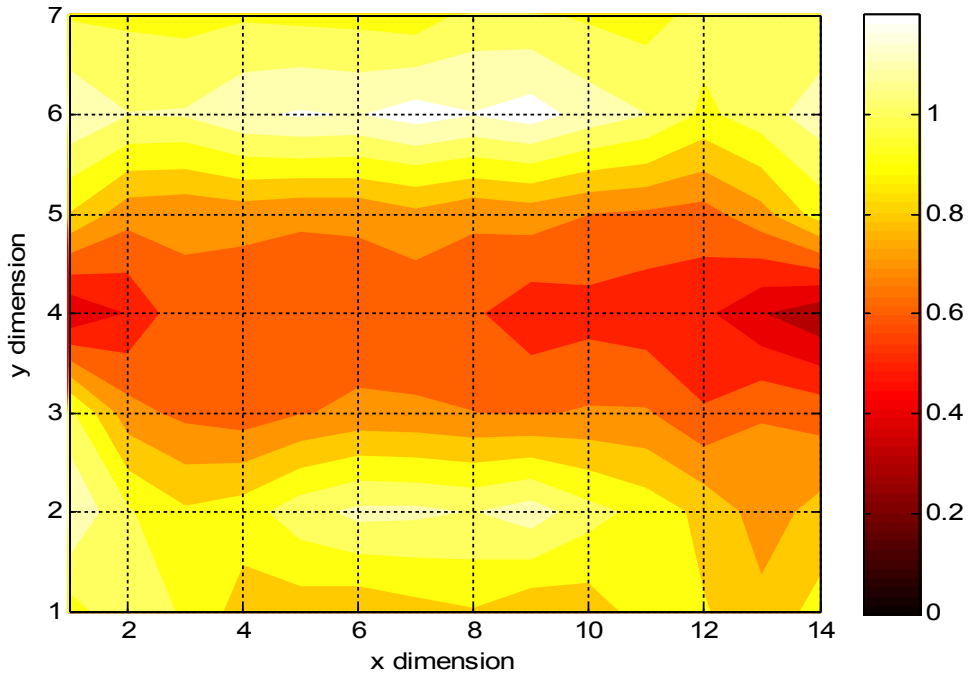

Figure 25: Normalized power coefficient for body shadowing in scenario 1 with a frequency bandwidth of 0.38 – 3.8 GHz and the antennas orientated vertically.

The body shadowing of scenario 1 with the same setup was also investigated with the antennas orientated horizontally. The normalized power coefficient is shown in Figure 27. Again when the main LOS path and ground path are obstructed the total received power is degraded. At the coordinates (4,7) the energy is again 60% of the power without body shadowing. The received energy does not exceed that without body shadowing, as is seen in Figure 25 with the vertical antenna orientation. The channel response at coordinates (4,7) is shown in Figure 26. The main LOS path and ground paths are attenuated. The first received path with body shadowing is 60% of the non obstructed.

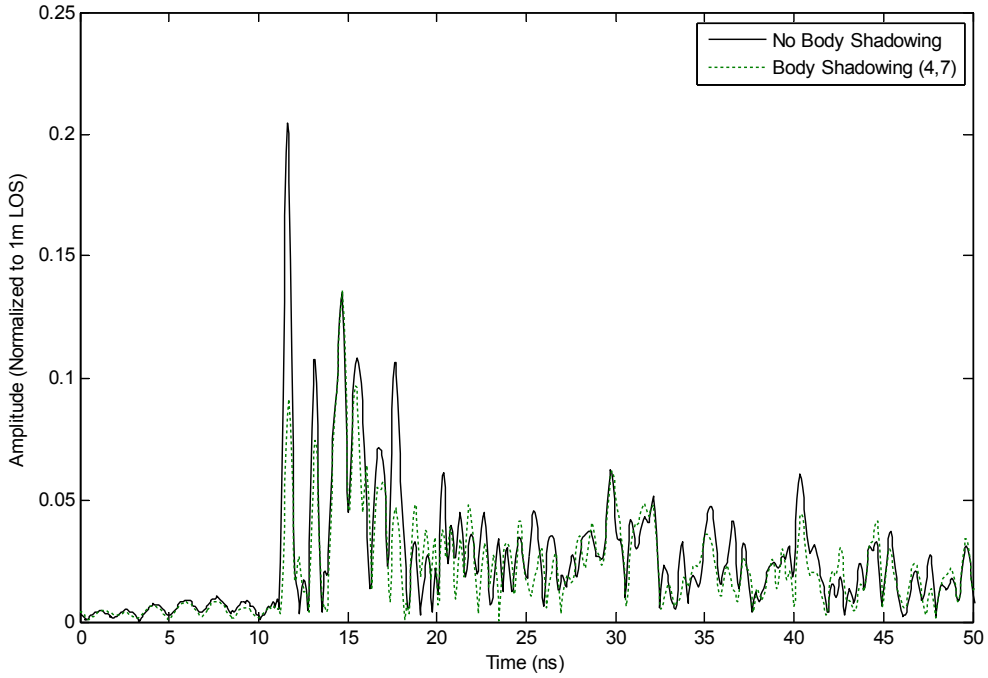

Figure 26: Correlation with and without body shadowing in scenario 1 of the received signal, with a bandwidth of 0.38 – 3.8 GHz and the antennas orientated horizontally.

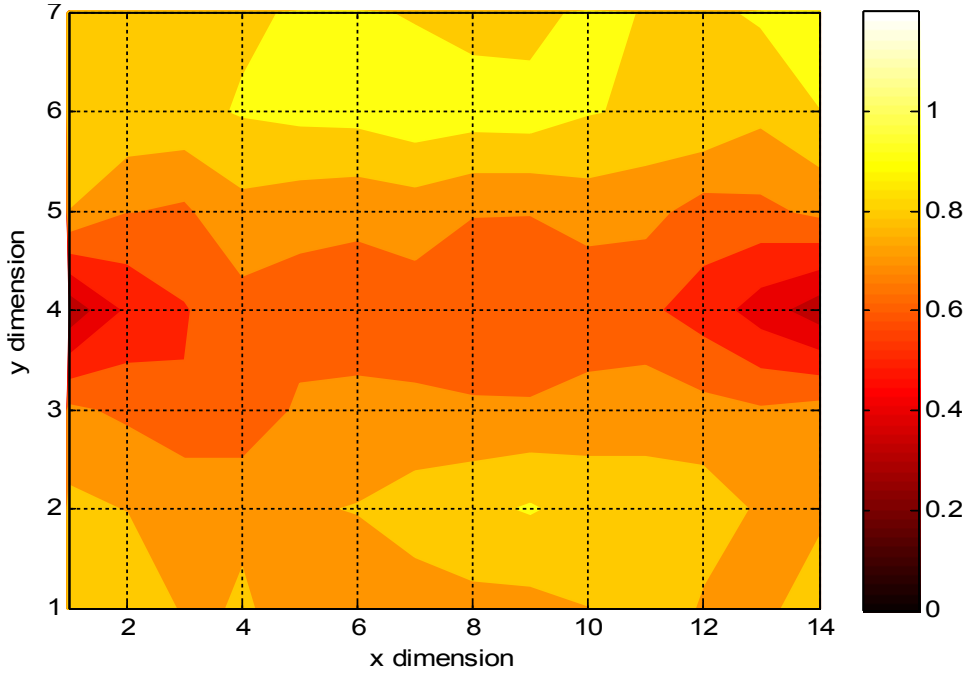

Figure 27: Normalized power coefficient for body shadowing, in scenario 1 with a frequency bandwidth of 0.38 – 3.8 GHz and the antennas orientated horizontally.

4.4.2 Body Shadowing 3.1 to 10.6 GHz

This section investigates body shadowing using the 3.1 to 10.6 GHz bandwidth with the antennas vertical and horizontal. The same setup is used, with the measurement performed in scenario 6 as shown in Figure 4. Scenario 6 is different from Scenario 1 in that the surrounding benches are covered with equipment. Also in scenario 6 the feet are close together in order to improve accuracy on the grid; however, this may attenuate the ground path more. The pulses in the time domain graphs are narrower, due to the larger bandwidth in the frequency domain.

The vertical antenna orientation is investigated first. Figure 28 shows channel responses with and without body shadowing. The body shadowed response for the first and second received signals are the main LOS and ground path signals. The shadowed response is slightly shifted by 0.13 nanoseconds due to the additional propagation delay

through the human body. There are other paths that can be seen that are not time delayed and are correlated very well to the unobstructed path, between 15 to 16, and 20 to 21 nanoseconds. These paths are not propagating though the human body as they are not delayed, and closely follow the unobstructed path response. The first and second body shadowed paths are 40% of the unobstructed paths. Figure 29 shows the normalized power contour, normalized to the unobstructed path. The energy at the middle of the LOS path at coordinates (4,7) is 35%. There is little loss when 0.6 meters away from the LOS path. The loss is higher than measured previously; this is expected because the frequencies are higher which results in less energy being received due to the interactions with the body.

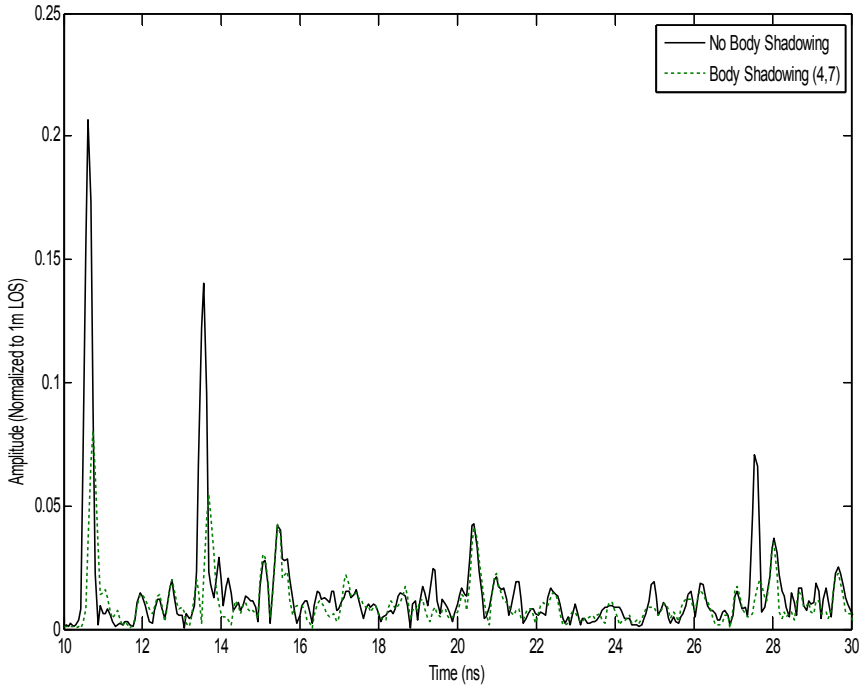

Figure 28: Correlation with and without body shadowing in scenario 1 of the received signal, with a bandwidth of 3.1 – 10.6 GHz and the antennas orientated vertically.

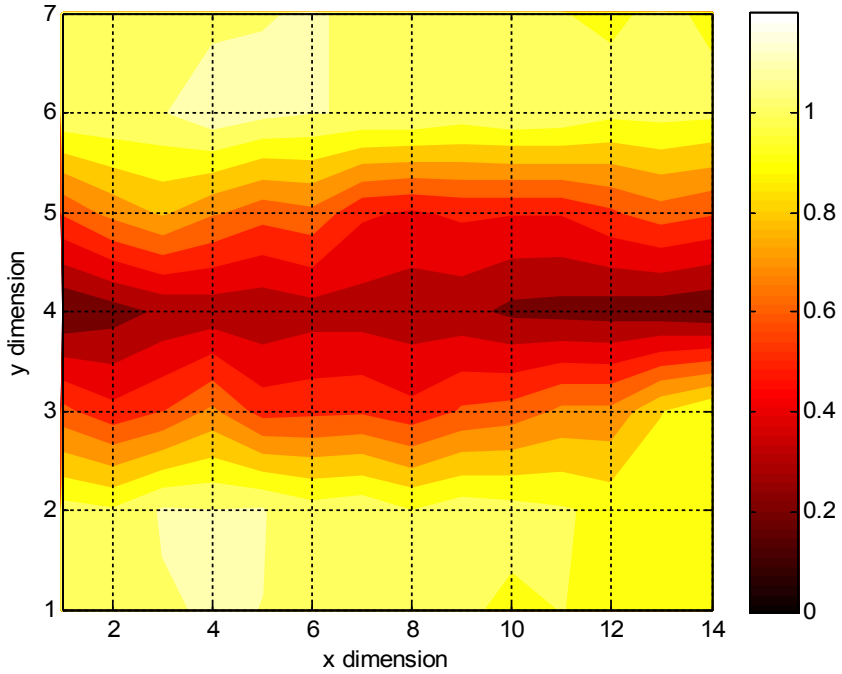

Figure 29: Normalized power coefficient for body shadowing, in scenario 1 with a frequency bandwidth of 3.1 – 10.6 GHz and the antennas orientated vertically.

The horizontal body shadowing is also investigated. Figure 30 shows the normalized power contour, normalized to the unobstructed path. The power at the middle of the LOS path, coordinates (4,7) is 18%. There is little loss when 0.3 meters away from the LOS path; some regions of the graph show higher losses, which is most likely due to the body shadowing obstructing a reflected signal.

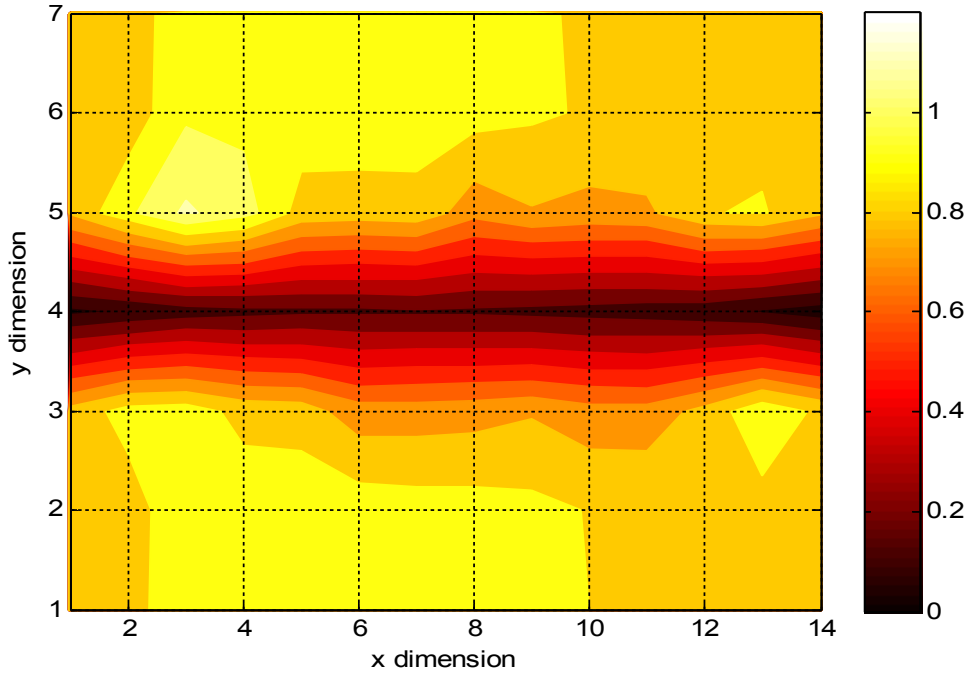

Figure 30: Normalized power coefficient for body shadowing, in scenario 1 with a frequency bandwidth of 3.1 – 10.6 GHz and the antennas orientated horizontally.

4.4.2.1 Body Shadowing RMS Delay Spread

The RMS delay spread was calculated for the various different body shadowing scenarios for both the horizontal and vertical antenna orientations. The RMS delay without body shadowing is shown in Table 14. Scenario 1 RMS delay varies significantly between the vertical and horizontal polarizations. Figures 24 and 26 show the channel response of the vertical and horizontal polarization, respectively. It can be seen from the channel responses that the distribution of power is spread out more over time with the antenna orientated vertically, and that the power is less spread with the antenna orientated horizontally. This is related to the environment of scenario 1, which has fewer desks and computers. In Scenario 6 the environment has the antennas surrounded in a horseshoe shape by benches and equipment. The closer proximity of the objects creates paths that are closer together for both the horizontal and vertical

polarizations.

Scenario	RMS Delay (ns)	
	Vertical	Horizontal
Scenario 1	19	16
Scenario 6	12	11

Table 14: RMS Delay without body shadowing at location (4,7) in Figure 23.

Scenario	RMS Delay (ns)	
	Vertical	Horizontal
Scenario 1	16	18
Scenario 6	15	13

Table 15: RMS delay with body shadowing at location (4,7) in Figure 23.

When body shadowing is introduced into the channel, the main LOS of path as well as the ground path are obstructed. This causes more emphasis to be put on the other multipaths and increases the RMS delay. This effect can be seen in Figures 31 through 34. In each of these cases, the mean delay also increases with body shadowing, as a result of the LOS path being removed. Prior results confirm this [3]. However, it was found that this is not always the case. Figure 31 shows that the RMS delay for the vertically polarized antenna decreased with body shadowing. Figure 24 shows the channel response with and without body shadowing.

In the majority of instances in Table 14 and 15, the horizontal polarization gave a lower RMS delay spread, except for the body shadowing in scenario 1 with vertical polarization. This may lead to potentially lower inter symbol interference with horizontal polarization as opposed to vertical, which is a function of the environment.

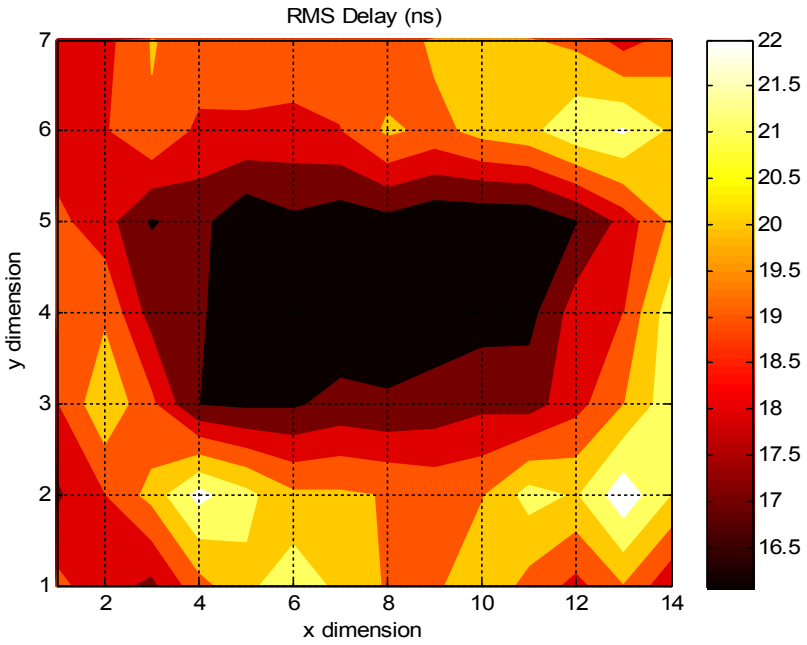

Figure 31: RMS delay spread with body shadowing in scenario 1 with a frequency bandwidth of 0.38 – 3.8 GHz and the antennas orientated vertically.

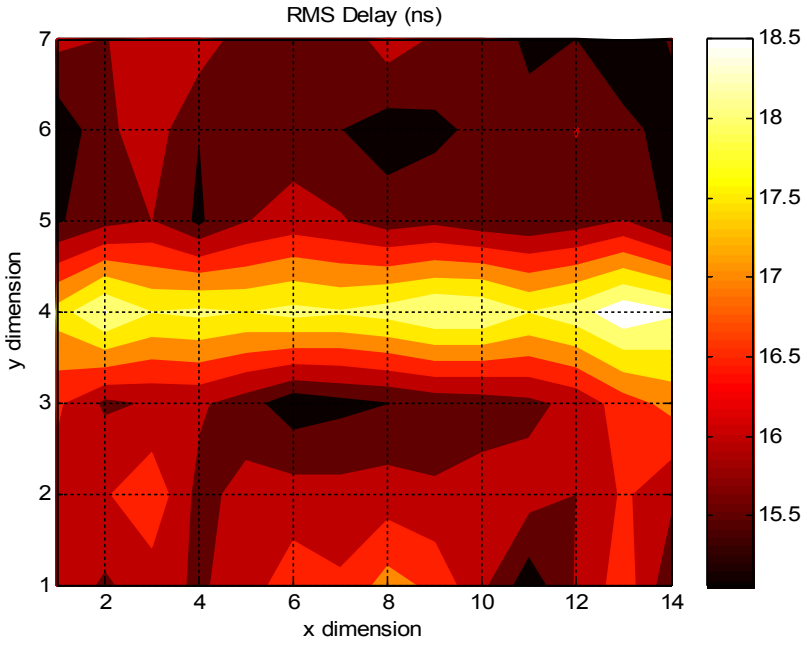

Figure 32: RMS delay spread with body shadowing in scenario 1 with a frequency bandwidth of 0.38 – 3.8 GHz and the antennas orientated horizontally.

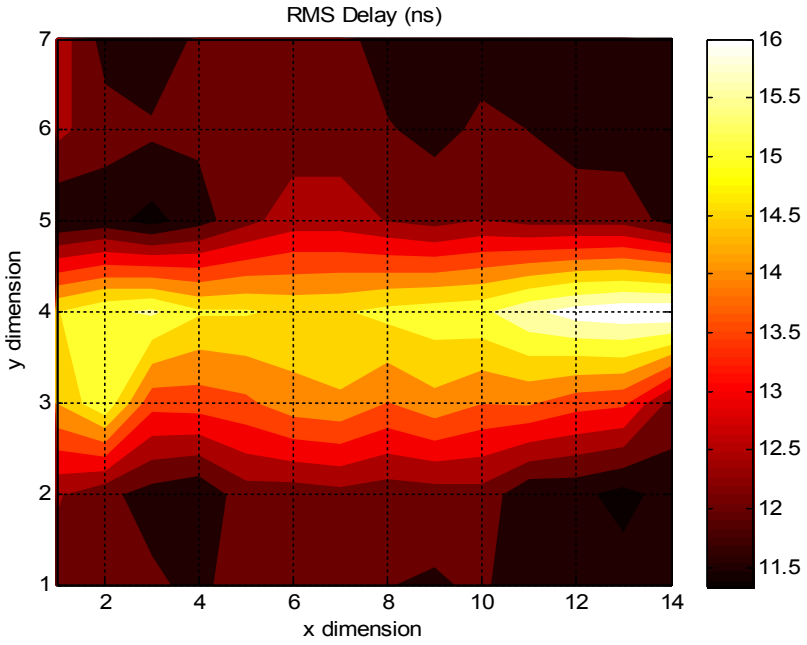

Figure 33: RMS delay spread with body shadowing in scenario 6 with a frequency bandwidth of 3.1 – 10.6 GHz and the antennas orientated vertically.

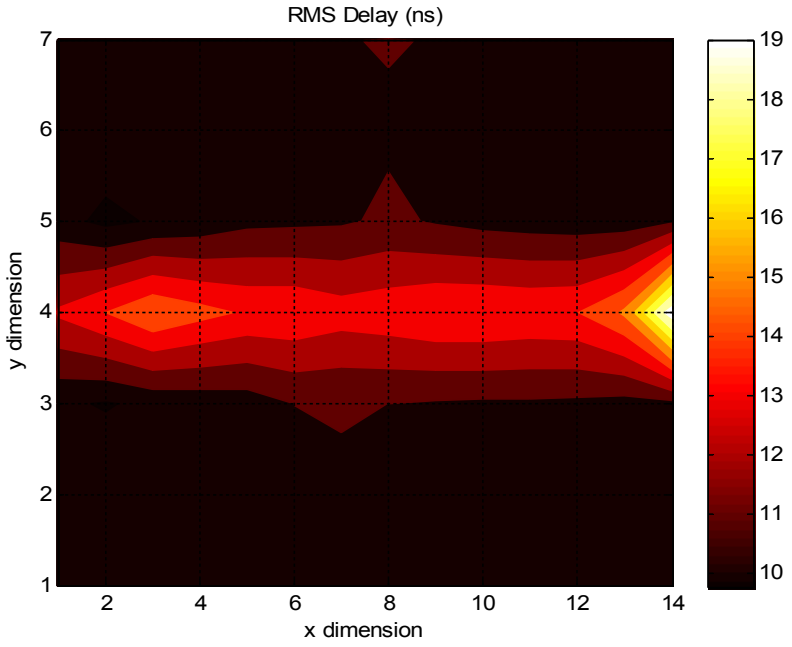

Figure 34: RMS delay spread with body shadowing in scenario 6 with a frequency bandwidth of 3.1 – 10.6 GHz and the antennas orientated horizontally.

4.5 Small Scale Fading

The spatial correlation is investigated in scenario 7 as shown in Figure 4. The transmit antenna is stationary during the measurement. Both antennas remain at a fixed distance off the ground. Both vertical and horizontal antenna orientations are investigated. The elevation off the floor for the vertical and horizontal antenna orientations is 1.5 and 1.3 meters, respectively. The receiving antenna is mounted to a Ryobi miter saw quickstand model # A18MS01. The sliding arms were used to move the antenna along the x axis. The quick stand is moved along the y axis when necessary. The spatial correlation is measured using a 2 meter LOS reference measurement. Two meters was used as opposed to the traditional one meter to reduce the near field antenna interactions between the transmit antenna and the metal quickstand. The mid frequency is typically used to determine the half wavelength grid spacing. However, since the bandwidth is very large

'3.1 to 10.6 GHz, a smaller spacing based on the highest frequency was used. A spacing of 1.5 centimetres was determined to be acceptable. 1.27 centimetres was used as it was a convenient spacing with the empirical units on the quickstand. The grid used was 1 meter by 3 centimetres.

Figure 35 shows the spatial correlation of the entire received signal for the vertically orientated antennas in a LOS environment in scenario 7. As can be seen, moving further away from the reference point (0, 200), is not always better, and the correlation oscillates with a damped decaying oscillation. The optimal separation in this environment is around 3 cm, which gives a spatial correlation of 60%. However, due to physical constraints of the antennas, a larger distance may be necessary.

Figures 36 through 38 show the fading based on the amount of energy that is captured in the receiver, by limiting the capture in the time domain. The figures show that as less multipath energy is captured, the oscillations diminish. If only a single path is captured as shown in Figure 39, the spatial fading does not oscillate as it does in a multipath environment. This is also a result of the large bandwidth of 3.1 to 10.6 GHz which provides a fine time resolution in the time domain and the ability to avoid any multipath fading.

Figure 36 shows the spatial correlation of the entire received signal for the horizontally orientated antennas in a LOS environment in scenario 7. As seen in the vertical orientation with minimal multipaths, the spatial correlation does not oscillate around the reference point. The horizontal channel in this environment has fewer multipaths. To achieve a spatial correlation of less than 60% requires a separation distance in the order of 0.4 to 0.5 meters.

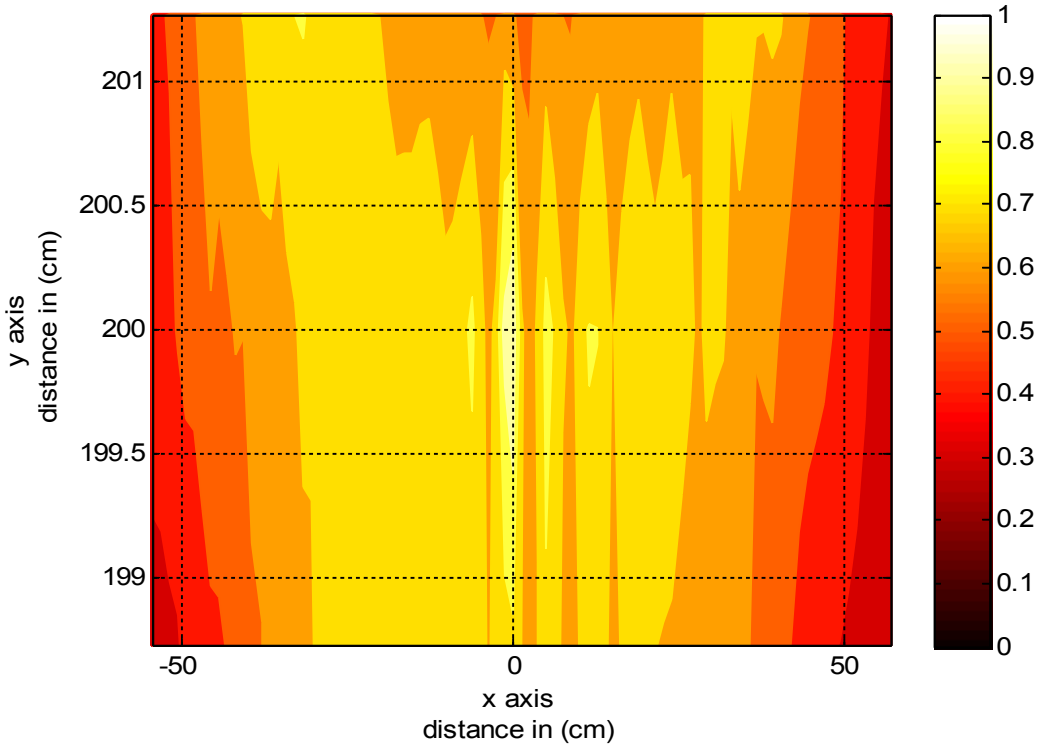

Figure 35: Spatial correlation at 3.1 – 10.6 GHz with antennas orientated vertically, total received signal.

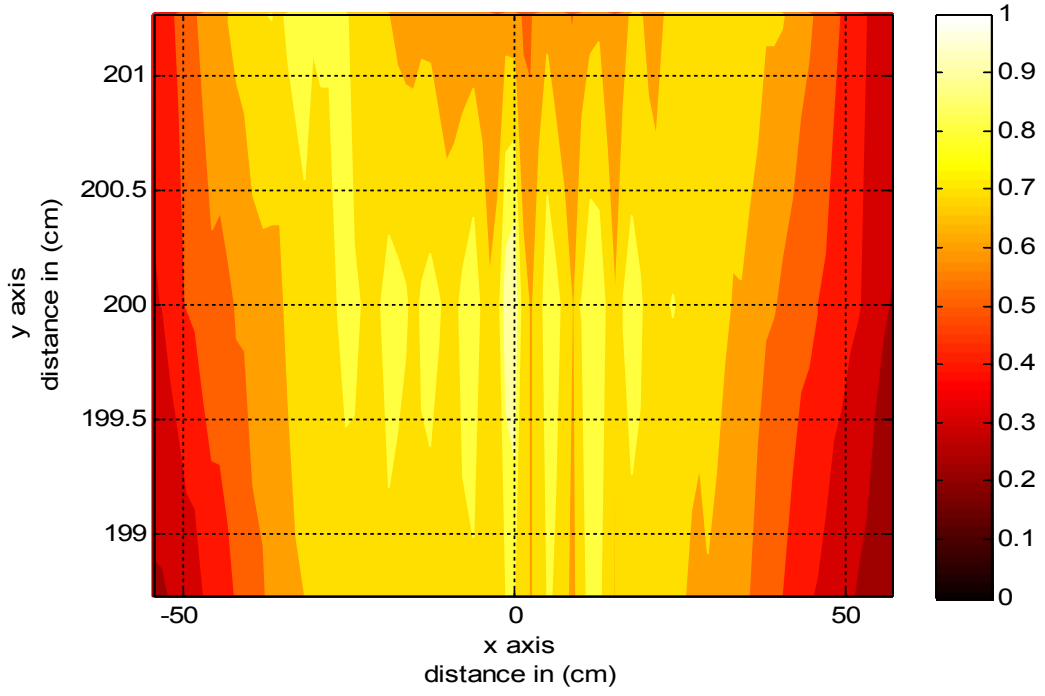

Figure 36: Spatial correlation at 3.1 – 10.6 GHz with antennas orientated vertically, first 20 nanoseconds of the received signal.

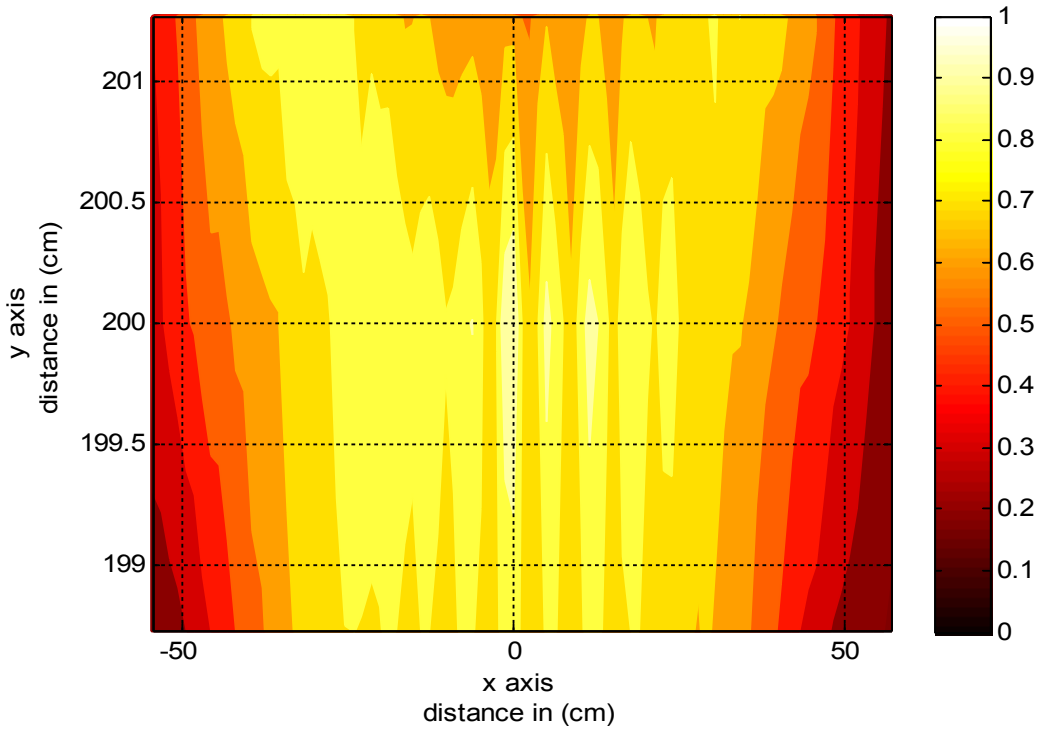

Figure 37: Spatial correlation at 3.1 – 10.6 GHz with antennas orientated vertically, first 10 nanoseconds of the received signal.

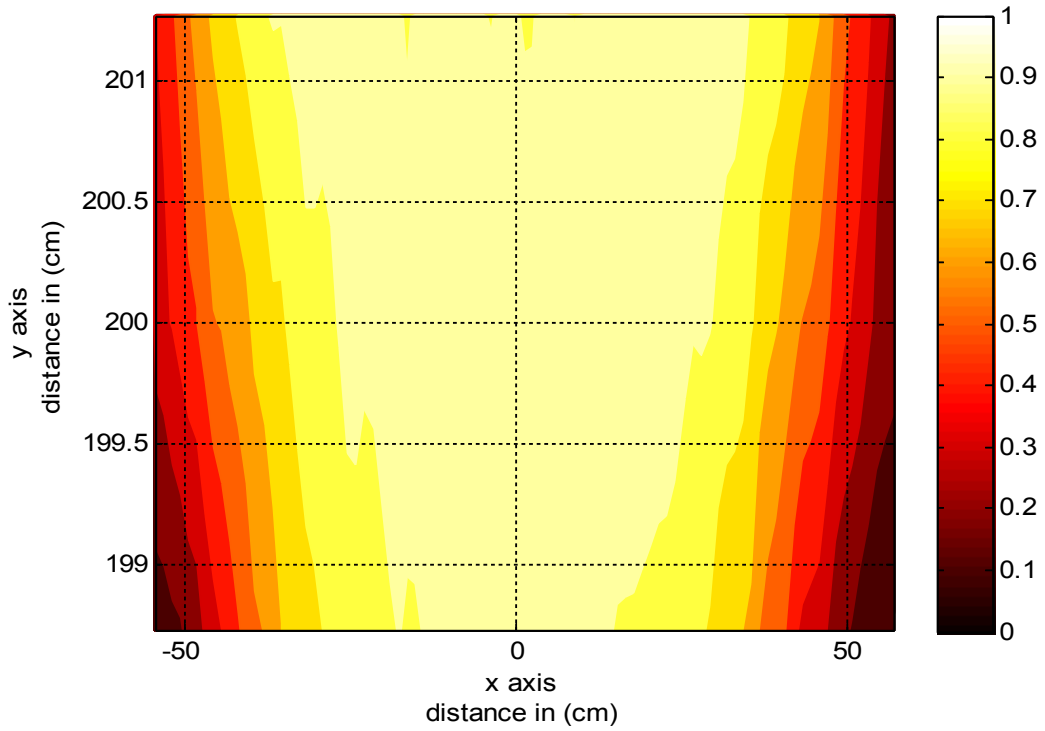

Figure 38: Spatial correlation at 3.1 – 10.6 GHz with antennas orientated vertically, first 3 nanoseconds of the received signal.

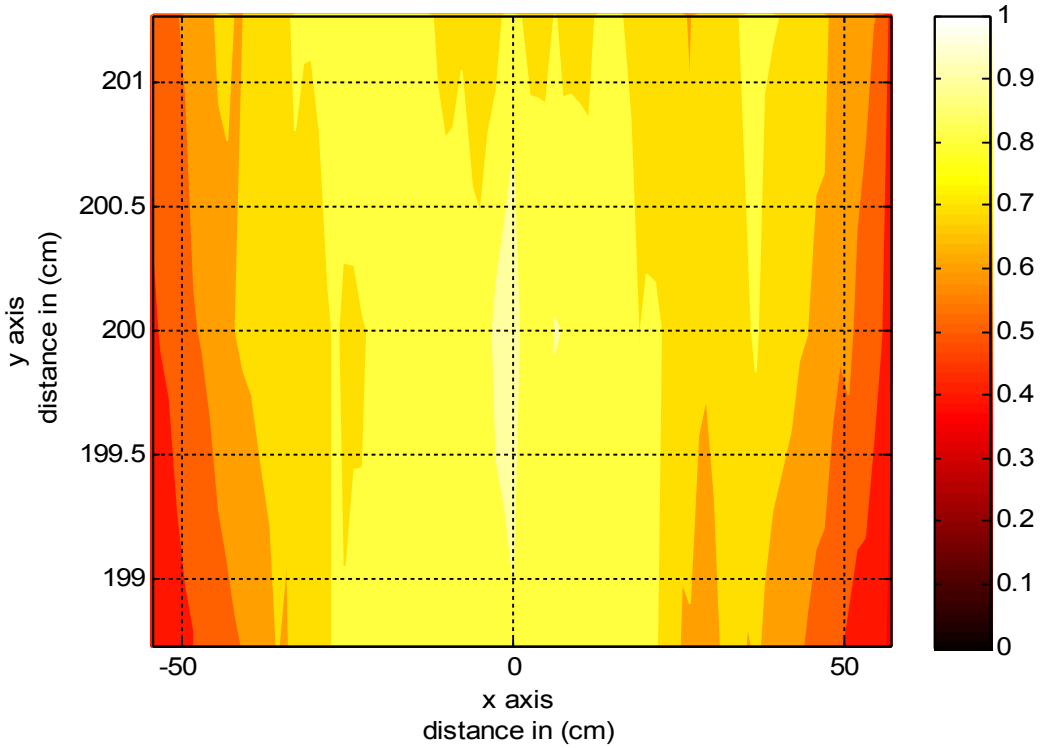

Figure 39: Spatial correlation at 3.1 – 10.6 GHz with antennas orientated horizontally, total received signal.

5 Conclusions, Practical Uses and Future Work

5.1 Conclusions

The UWB channel response was investigated in an indoor office environment, using the frequency domain method in the 3.1 to 10.6 GHz bandwidth. Different LOS and NLOS scenarios were investigated. The reciprocity, body shadowing and spatial correlation were measured. In each of these cases, the horizontal and vertical antenna polarizations were compared.

The reciprocity of several LOS and NLOS scenarios were investigated. Measurements were performed in excess of 10 meters, with significant losses and multipaths. There were no notable differences in the reciprocity using horizontal or vertical polarizations. The reciprocity for a horizontal or vertically polarized wave forms were found to be highly correlated, better than or equal to 97%.

The path loss in the same environments were calculated using the path loss coefficient (15). In a LOS environment, the coefficient varied between 1.9 to 2.4. There was no significant difference between the horizontal or vertical polarizations. The expected path loss is 2; however, there was more variance than expected. In a NLOS environment, the horizontal or vertical polarizations were investigated. In 70 percent of the scenarios, the horizontal polarization had slightly less loss than the vertical. More measurements at different office buildings are required before a more generalized and conclusive result can be determined between the path loss of vertical and horizontal polarized antennas in the indoor office environment.

Body shadowing was investigated in two different scenarios, using a two dimensional

grid with different bandwidths. A scenario that was previously investigated in [3] using the time domain, with a pulse with a 10 dB bandwidth of 0.38 to 4 GHz was compared. The power loss measured in [3] at the center of the grid was 10 percent. Re-performing this in the frequency domain showed that the center of the grid power loss was 40% for both horizontal and vertical polarizations. The differences are related to the differences between the time domain and frequency domain measurements. It is also possible that some of the differences are a result due to inconsistencies between the humans that were used for body shadowing. At the higher frequencies and bandwidths of 3.1 to 10.6 GHz, the power loss at the center of the grid varied significantly between the horizontal and vertical polarizations. For the horizontal and vertical polarizations, the path loss at the center frequency was 82% to 65%, respectively. The RMS delay spread with and without body shadowing was also investigated. In the two scenarios investigated, the horizontal polarization had less RMS delay spread than the vertical polarization. A smaller RMS delays spread indicates lower inter symbol interference.

The spatial correlation on a two dimensional grid in a LOS environment was investigated. It was found that as less multipath energy is captured, the oscillations of the spatial correlations decrease. For multiple receive antennas, in a MIMO environment, antennas that are poorly correlated can be used to create independent spatially separated channels. It was found that in the scenario investigated the horizontal polarization had less multipaths than the vertical polarization. As a result, vertical polarization had minimas in the spatial correlation plots that are better suited for multiple antennas with spatially independent channels.

5.2 Practical Use of Results

The results presented in this thesis can be used for practical system design. This thesis looked at channel measurements in the indoor office environment, using the frequency domain from 3.1 to 10.6 GHz; and compared vertical and horizontal polarized waveforms.

For path loss, there was no significant difference for LOS between the polarizations. The LOS varied from 1.9 to 2.4. For NLOS, the horizontal had slightly less path loss most of the time. Worst case measurements showed a NLOS path loss up to 5.6 for a heavily attenuated multipath environment. The path loss can be calculated using Equation (15).

The channel was found to be highly reciprocal in all the scenarios. This means that the received impulse response can be used as a prefilter to spatially focus the transmitted signal, and reduce the number of taps that the receiver needs to have to capture the multipath energy.

The channel was found to be significantly impacted by human interaction. If the system is relying on LOS channels, the performance of the system will be significantly impacted. Budget for around 65% power loss for vertical orientations and 82% for horizontal at the center of the channel. If the system is not relying on LOS communications, the power loss can still be significantly impacted if the body shadowing is close to either antennas. Because of this, it is highly recommended that multiple transmit and receive antennas are used to reduce the affects of body shadowing. An antenna spacing around 30 cm would be acceptable to reduce the impact of body shadowing, see Figures 29 and 30.

Spatial fading was investigated in a LOS environment, with reflections off the surrounding environment. Ultra wide band is different from traditional narrow band systems, as the larger bandwidth means that it is able to resolve smaller differences in time, in the time domain. This makes UWB immune to fading. Due to multipaths, spatially separate channels can be created. If the environment does not have sufficient multipaths, or if the number of captured multipaths is small due to a simpler receiver design, the desired spatially separate channels may not be created. An alternative would be to use orthogonal polarizations, such has horizontal and vertical to create separate channels, which could be used to reduce the affects of body shadowing.

5.3 Future Work

1. The measurements in this thesis did not investigate the reciprocity at various different antenna elevations, and polarization angles in a NLOS environment. In an office environment, the end users of a system may place and orient antennas in a variety of conditions. Further investigations into this could be conducted to confirm the reciprocity under these conditions.
2. Body shadowing could be further investigated, as there were some discrepancies between the body shadowing performed in [3] and in this thesis. The differences in results inpart may be related to the differences between the humans used, as well as the belongings carried. A study of UWB body shadowing with humans of different shapes, sizes, and belongings carried would provide data that could be used for determining how these affect the channel's response.
3. The UWB channel's response with vertical polarization has been investigated by multiple research groups. Horizontal polarization in the office environment has

not. Further investigation into path loss, body shadowing, spatial correlations in other indoor office environments would help provide better models for UWB propagation with horizontal polarization. This thesis has found that the horizontal polarization has less multipaths than vertical. Further measurements in other office environments are required to confirm this.

Bibliography

[1] "Revision of part 15 of the commission's rules regarding ultra-wideband transmission systems," First note and Order, Federal Communications Commission, ET-Docket 98-153, Apr. 2002, http://transition.fcc.gov/Bureaus/Engineering_Technology/Orders/2002/fcc02048.pdf (last visited Nov. 2012).

[2] J. Sangthong, S. Promwong, P. Supanakoon, "Comparison of UWB fingerprinting with vertical and horizontal polarizations for indoor localization," Proc. of ETCI-CON, pp.588-592, May 2010.

[3] R. Zhang, L. Cai, S. He, X. Dong, J. Pan, "Modeling, validation and performance evaluation of body shadowing effect in ultra-wideband networks," Physical Comm., Vol. 2, No. 4, pp. 237-247, Dec. 2009.

[4] S. He, Ultra wideband channel measurement and transmit reference pulse cluster receiver prototype implementation, M.A.Sc. disertation, Dept. of ECE, Univ. of Victoria, Victoria, B.C., Canada, 2009.

[5] P. Zakharov, A. Babushkin, A. Korolev, A. Kozar, "Impact of bandwidth, center frequency and spatial position on the result of ultra-wideband power delay profile measurement and accuracy of predictions," IEEE Int'l. Symp. on Microw., Antenna, Propag. and EMC Tech. for Wireless Comm., pp.1094-1099, 2009.

[6] Z. Irahhauten, A. Yarovoy, G. Janssen, H. Nikookar, L. Ligthart, "Ultra-wideband indoor propagation channel: measurements, analysis and modeling," EuCAP 2006, pp.1-6, Oct. 2006.

[7] C. Chong, Y. Kim, S. Lee, "UWB indoor propagation channel measurements and data analysis in various types of high-rise apartments," Proc. of IEEE Vehicular Tech. Conf., pp.150-154, Sep. 2004.

[8] M. Koiwai, T. Kobayashi, "Effects of location and room height on ultra wideband propagation around the human body," IEEE APS Topical Conf. on Antennas and Propag. in Wireless Comm., pp.1314-1317, Sep. 2011.

[9] J. Wang, I. Kimura, Q. Wang, "UWB on-body channel measurement and BER performance in an indoor environment," Proc. of the 3rd European Wireless Tech. Conf., pp.57-60, 2010.

[10] T. Zasowski, G. Meyer, F. Althaus, A. Wittneben, "UWB signal propagation at the human head," IEEE Transactions on Microw. Theory and Tech., Vol. 54, No. 4, pp. 1836-1845, Apr. 2006.

[11] J. Reed, C. Anderson, A. Annamalai, A. Attiya, N. August, M. Buehrer, W. Davis, M. Gong, S. Griggs, D. Ha, J. Ibrahim, S. Licul, S. Midkiff, S. Muthuswamy, J. Neel, W. Tranter, *An Introduction to Ultra Wideband Communication Systems*, Prentice Hall, Indiana, USA, 2005.

[12] H. Schantz, "Introduction to ultra-wideband antennas," Proc. IEEE Conf. Ultra Wideband systems and Technologies, pp.1-9, Nov. 2003.

[13] D. Ghosh, A. De, M. Taylor, T. Sarkar, M. Wicks, E. Mokole, "Transmission and reception by ultra-wideband (UWB) antennas," IEEE Antennas Propagat. Mag., Vol. 48, No. 5, pp. 67-99, Oct 2006.

[14] T. Rappaport, *Wireless Communications: Principles and Practice*, Prentice Hall, USA, 1996.

[15] A. Goldsmith, *Wireless Communications*, Cambridge University Press, USA, 2005.

[16] R. LaMaire and M. Zorzi, "Effect of correlation in diversity systems with rayleigh fading, shadowing and power capture," IEEE J. Selected Areas in Communications, Vol. 14, No. 3, pp. 449-460, Apr. 1996.

[17] Agilent Network Analyzer Basics, Agilent Technologies Ltd., USA, Aug. 2004, http://cp.literature.agilent.com/litweb/pdf/5965-7917E.pdf (last visited Nov. 2012).

[18] J. Foerster, E Green, S. Somayazulu, D. Leeper, "Ultra-Wideband Technology for Short- or Medium-Range Wireless Communications," Intel Technology Journal Q2, Vol. 1, No. 1, pp. 1-11, 2001.

Appendix A: Measurement Equipment

The equipment used to measure the channel impulse response using a vector network analyzer is shown below. Figure 3 shows a block diagram of the setup. The list of equipment used is given in Table 16 and Table 17. The equipment is listed in order of the propagated signal path, from the network analyzer to the transmit antenna, and the receive antenna back to the network analyzer. Table 16 lists the equipment from the network analyzer to the transmit antenna, and Table 17 lists the equipment from the receive antenna to the network analyzer. The configuration parameters for the network analyzer are show in Table 18.

Description	Model Number
Network Analyzer	Agilent Tech. N5230A
RF Coax Cable (10 ft)	Minicircuits CBL-10FT-SMSM
RF Coax Cable (6 ft)	Minicircuits CBL-6FT-SFNM
Omni directionalAntenna 2-18GHz	Electrometrics EM-6865

Table 16: Equipment from the network analyzer to the transmit antenna.

The antennas used are omni-directional antennas. The manufacture's antenna patterns for the azimuth and elevation are shown in Figure 40 and Figure 41. The gain versus frequency is shown, Figure 42. As can be seen, the gain is fairly constant across the frequency band of interest, 3.1 to 10.6 GHz.

Description	Model Number
Omni directionalAntenna 2-18GHz	Electrometrics EM-6865
RF Coax Cable (6 ft)	Minicircuits CBL-6FT-SFNM
RF Coax Cable (10 ft)	Minicircuits CBL-10FT-SMSM
LNA 25dB 0.5 to 26. GHz Amplifier	Agilent 83017A
RF Coax Cable (1.5 ft)	Minicircuits CBL-1.5FTSMSM
Network Analyzer	Agilent Tech. N5230A

Table 17: Equipment from the receive antenna to the network analyzer

Network Analyzer Parameter	Settings
Start Frequency	3.1 GHz*
Stop Frequency	10.6 GHz*
Averaging	10
Sweep Type	Stepped
Sweep Points	1601 or 16001
Sweep Time	16.9ms or 169ms, depending on points
IF Bandwidth	100 kHz
Attenuation	Auto
Power Level	0 dBm
Measurement	S_{21}
Calibration	Through
Time Domain Start Time	0 ns
Time Domain Stop Time	100 ns

* Frequency band of 0.38 to 3.8 GHz was also used in some measurements

Table 18: Network analyzer's setup.

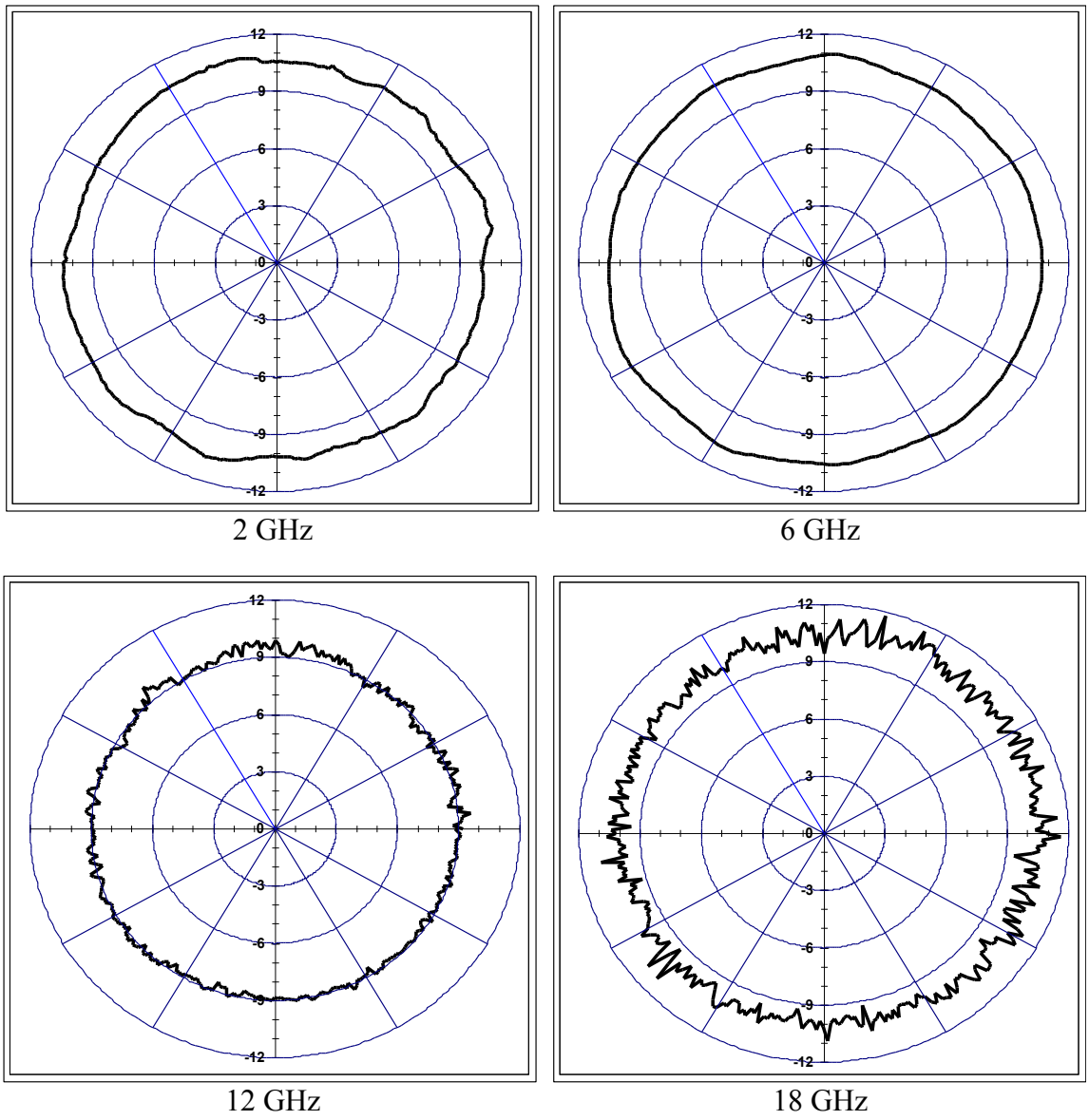

Figure 40: EM-6865 Azimuth Patterns

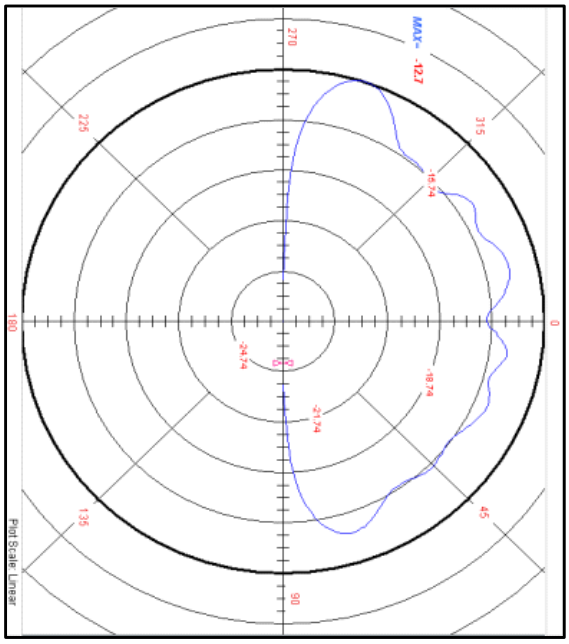

2 GHz

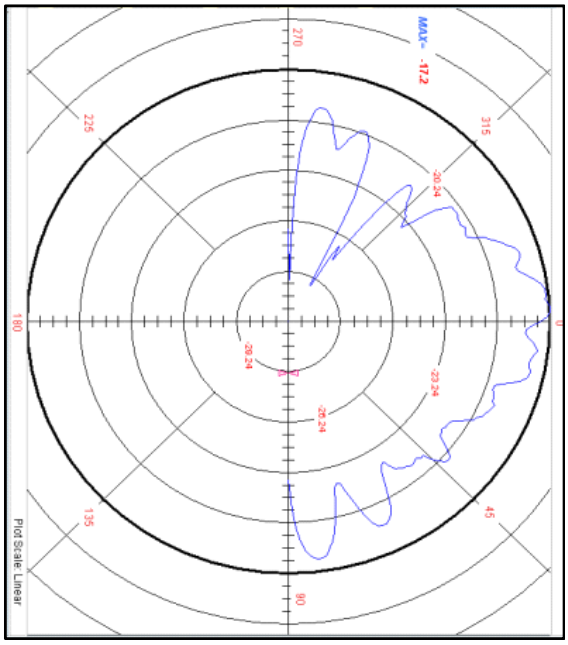

6 GHz

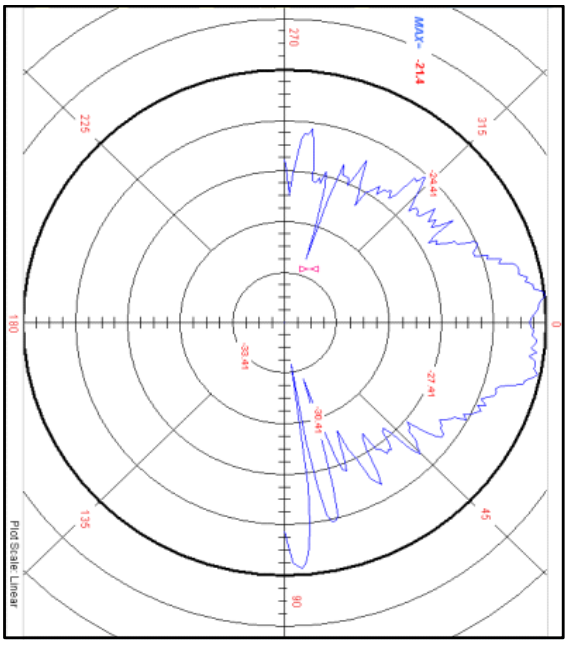

12 GHz

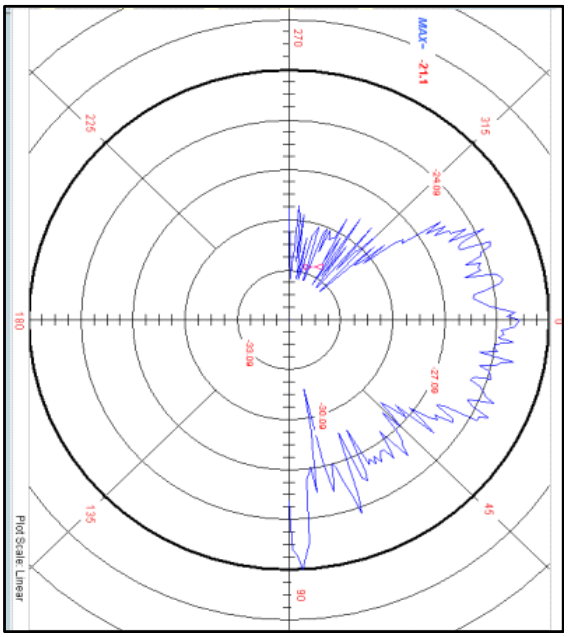

18 GHz

Figure 41: EM-6865 Elevation Patterns

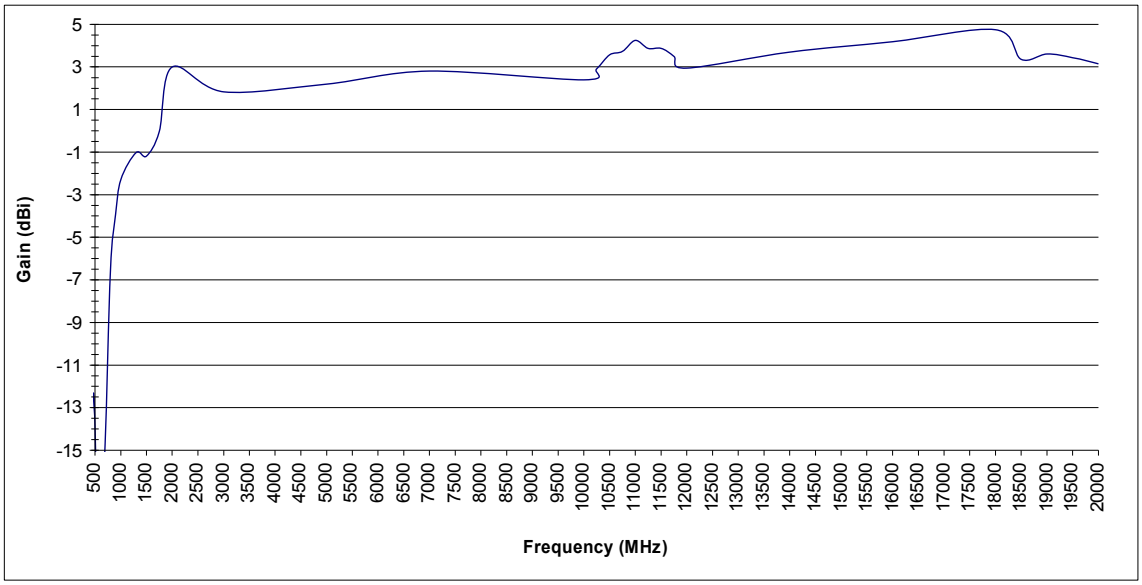

Figure 42: EM-6865 Gain